



Decline of Lanna ceramic group production in northern Thailand (Ban Bo Suak site) confined by radiocarbon and luminescence dating

Prapawadee Srisunthon¹ · Daniela Mueller¹ · Frank Preusser¹

Received: 31 January 2022 / Accepted: 3 July 2022 / Published online: 18 July 2022
© The Author(s) 2022

Abstract

The Lanna group is a traditional ceramic production style from Southeast Asia, with several kiln sites found distributed all over present northern Thailand. However, its origin and development are considered controversial and chronological constraints are scarce. Applied here are radiocarbon dating to charcoal remains and luminescence dating to ceramics, kiln wall material, and fluvial sediments from the Ban Bo Suak archaeological site near Nan, northern Thailand. The site has been suspected to have been abandoned due to destruction by a flood. Unexpectedly, the ceramic samples lack proper thermoluminescence signal properties and only two samples could be dated using optically stimulated luminescence (OSL). These ages in combination with published radiocarbon ages point towards a ceramic production around AD 1700. The kiln wall material and fluvial sediments reveal evidence for partial resetting of the OSL signal, which is unexpected for heated material. Supported by some radiocarbon ages, the OSL ages imply a temporal connection between the last use of the kilns and the flood deposits, during the fifteenth century AD. Besides general methodological considerations, the data reported here indicates that while a flood apparently dismantled several kiln sites, this did not stop the production of Lanna style ceramics in the region.

Keywords Lanna kilns · Ceramic production · Radiocarbon dating · Luminescence dating · Thailand

Introduction

Developments in the characteristics of ceramic stoneware technology in Southeast Asia deliver valuable perspectives with regard to the prehistoric evolution (Reynolds, 1992; Higham and Rispoli 2014; Sarjeant 2014) as well as to the deciphering of social, political, and economic changes during the historical period (Grave 1995; Grave et al. 2000; Low 2004). A critical point is the accurate dating of ceramic technologies using chronometric dating techniques. An alarming example in this context is the radiocarbon dating of charcoal found in a soil layer associated with a stoneware assemblage at Spirit Cave, northern Thailand, that was originally interpreted to reflect an early cultural development during the transition from hunter-gatherer to farming communities around 5500 BC (Gorman 1970; Higham 1989). It was later shown by the radiocarbon dating of organic resin attached

to the ceramics that the pottery is actually much younger (Lampert et al. 2003). This highlights the need to carefully consider if a radiocarbon age does in fact reflect the age of the event, i.e., the time of manufacture or the last use (cf. Casanova et al. 2020). The general problem is that older or younger organic matter can be added into the archaeological context through sediment reworking by bioturbation (e.g. Zuo et al. 2016), for example by roots or insects, and anthropogenic activities such as resettlement and deforestation (e.g. Lechterbeck et al. 2014).

Due to the problems discussed above and the fact that material suitable for radiocarbon dating has a poor preservation potential under tropical climate conditions (Storm et al. 2013), different luminescence techniques represent alternative approaches in the context of dating archaeological finds (cf. Liritzis et al. 2013). Initially, thermoluminescence (TL) was proposed for the dating of pottery (Aitken et al. 1964) and the methodology was later adopted for the dating of heated objects such as kilns (e.g. Aitken 1985; Zacharias et al. 2006; Zander et al. 2019). With the advent of optically stimulated luminescence (OSL) dating (Huntley et al. 1985),

✉ Prapawadee Srisunthon
ps493@geologie.uni-freiburg.de

¹ Institute of Earth and Environmental Sciences, University of Freiburg, Freiburg, Germany

which uses a signal that is rapidly reset by daylight, direct dating of sediments embedding archaeological remains became feasible (cf. Roberts et al. 2015).

Both TL and OSL are based on electrons trapped at defects within the crystal lattice of quartz and feldspar minerals, which act as natural dosimeters (e.g. Aitken 1985, 1998; Preusser et al. 2008). During burial, the minerals absorb energy from ionizing radiation of the surrounding material and with time more and more electrons are trapped at the lattice defects. The latent TL and OSL signal grows proportional to time and the sample specific radiation level. The term luminescence refers to the light emitted from minerals during stimulation by either heat (TL) or light (OSL). To obtain a luminescence age, two parameters have to be determined. These are the amount of dose (radiation energy per mass) absorbed since the event to be dated, also known as equivalent dose (D_e , in the unit $\text{Gy} = \text{J kg}^{-1}$), and the level of ionizing energy acting on the sample with time, known as dose rate (Gy a^{-1}).

The focal point of this study is located in the Nan region, an intermountain basin in northern Thailand, situated between the Phi Pan Nam Range in the west and the Luang Prabang Range in the east (Fig. 1). The central part of Nan is characterised by the meandering river course and the associated floodplain of the Nan River, which fostered the growth of local communities. During historic times, Nan was initially an independent kingdom that was established in the thirteenth century AD to govern multi-ethnic groups, especially the highland tribes (Cheewinsiriwat 2013). The kingdom was forced to join the Lanna Kingdom in the fourteenth century and later the Siamese Kingdom (modern Thailand) in the seventeenth century AD. According to the distribution of archaeological sites, the Nan region shares similarities with other northern Thai ancient cities, and is characterised by a linear settlement pattern along rivers, as these acted as transportation lines and ensured constant water supply (Boomgaard 2007; Ng et al. 2015). However, due to their location along the river courses, Nan settlements have been

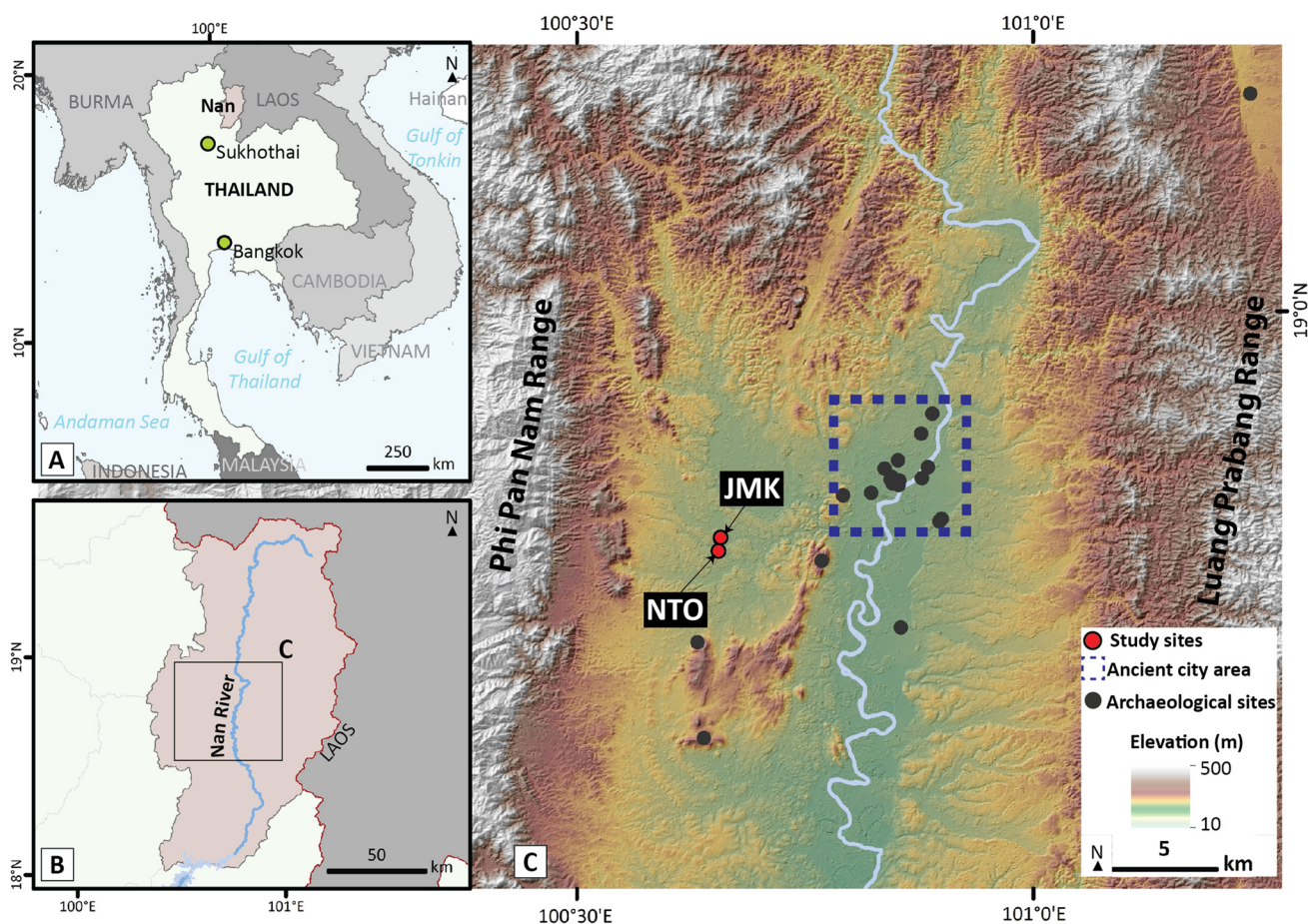


Fig. 1 A Location of the province of Nan in northern Thailand. B Position of the wider study area in the center of the Nan region. C Digital Elevation Model (DEM) of the Nan Valley showing the location of individual kiln sites JMK and NTO near Ban Bo Suak village.

The area within which Nan city was relocated several times is indicated, as well as the position of important archaeological sites (DEM derived from TanDEM-X 2016 with 11 m resolution and defined projection using WGS1984 zone 47 N coordinator system)

at high risk from seasonal flooding that regularly occur during the monsoon period (currently May till October). In fact, historic records document that during the period AD 1368–1818, the main city of Nan was several times severely destroyed by floods and had to be relocated to other parts of the valley plain (Pharitdet 1918; Boonyai 2008; Chairat 2009). One of these flood events appears contemporary with the period when the ceramic production site at Ban Bo Suak village (Fig. 1C) was abolished, as the site is covered by flood sediments. This site comprises glazed stoneware ceramics and a well-preserved kiln complex, representing the adaptation of techniques developed in China (Hein et al. 2004). From the location and typology, it is believed that the production was active during the period of the Lanna Kingdom (thirteenth–seventeenth century AD) and it resembles the well-known ceramics from Si Satchanalai of Sukhothai (Hein 2008; Praicharnjit 2011). However, the origin and development of this site and the entire Lanna ceramic group are considered controversial (see below).

The aim of this study is to provide additional chronological data for the Ban Bo Suak archaeological site and, through this, to contribute to the open scientific questions surrounding the Lanna ceramic group. The approach applied here is fourfold. First, charcoal material associated with the ceramics was dated using radiocarbon and the results are analysed with regard to plausibility. Second, it was attempted to date pottery directly using both TL and OSL. Third, the material taken from the kiln walls by the inner side of the firebox of three kilns was dated using OSL to determine the date of last use. Fourth, fluvial sediments covering both kiln structures and pits filled with pottery were dated by OSL. The fluvial sediment was used to determine the age of the natural hazard (flood) which might buried the pottery production site. By doing so, we expect to unveil the relationship between the flood deposits and the decline of the pottery production. Besides the implications for the human history of the Nan region and potentially the wider geographic context, this study highlights in particular several aspects that call for general caution when applying the presented methodology in similar archaeological settings. While some of these aspects have been reported in previous studies, some are described here for the first time. Hence, presented here is a case study that highlights problems and pitfalls associated with rather well-established methods routinely used in archaeological research.

Archaeological context

Information concerning the origin of the Lanna ceramic group is considered controversial since available data is only fragmentary. However, it appears that the emergence of pottery production might be related to trading and the migration

of potters from southern China to the Lanna region in present-day northern Thailand (e.g. Srisuchat 1996; Miksic 2006; Sukkham 2018). Pottery production was apparently firstly conducted in the Sukhothai area (Fig. 1A) in the late twelfth century AD (Rajanubhab and Crosby, 1919; Graham 1922; Le May 1933; Hein et al. 2004). This theory is supported by the observation that Lanna ceramic products share similarities with the technology widely applied in southern China around the tenth century AD, i.e. high-fired-glazed stoneware and the use of the “dragon kiln” type (Stargardt 2014). It has to be noted that the ceramics produced at Lanna and Sukhothai kiln sites are distinguished into two different group styles based on typology, although it is believed that the manufacture period was temporary (e.g. Shaw 1984). Both group styles share similar techniques, for example, wiping the glaze at the mouth rim and placing mouth-to-mouth rim-to-rim in the kiln while firing (Thansawang-dumrong 2005). However, each site of Lanna and Sukhothai group styles also has their own special characteristics. The ceramics from the Ban Bo Suak kiln complex seem similar to those from Ban Ko Noi in Sukhothai, as the same type of kilns was used and primarily glazed stoneware was produced. In the Ban Bo Suak kilns, mostly green glazed wares were produced with an outstanding imprinted motif, especially green glazed dishes with a fish imprinted motif (Supplementary Figure 1A). The glazed ware produced at this site is of a creamy, quite pale green. Only a few ceramics painted with flower motifs were (Supplementary Figure 1B). At Ban Ko Noi, brown-green glazed ceramics with a more intense colour than at Ban Bo Suak were produced (Supplementary Figure 1C). The dishes produced at Ban Bo Suak have a quite flat rim towards the outside, whereas the dishes from Ban Ko Noi are rounder and the rim extends inside. In addition, a black painting pattern is typically for ceramics from the latter (Supplementary Figure 1D). For the ceramic style of Ban Bo Suak, imprinting techniques were used or an extra pattern for the decoration was added; especially in the upper parts of the jar, patterns of owls and lotus have been recognised as typical (“Nan Pattern”; Supplementary Figure 2A). In contrast, the glazed jar style from Ban Ko Noi shows a vivid green colour but lacks decoration pattern and only sometimes the potter drew a line to decorate the item (Supplementary Figure 2B).

Shaw (1984) and Brown (1988) agree that the production of Lanna ceramics began in the thirteenth century AD. However, both authors assume that the ceramic production was already practiced in the area by the local Mon tribe before adopting Chinese ceramic styles and developing it further. Mon ceramics present various types: flat bottomed bowls and jars with assorted colours as well as light to dark green and brown or black items but only glazed on the inside. The theory of early Mon ceramic production is supported by the used firing technique, wherefore stoneware is stacked in a

chamber and laid out base-to-base or rim-to rim before firing. For the ceramic production at Ban Bo Suak, an engobe (slip) process that uses kaolin or high-clay slurry coating was applied. For this, the dry ceramic is coated to conceal defects on the surface before the glaze layer is applied (Bó et al. 2014). This process is a typical practice observed at Lanna kilns, especially those found in Nan and Sukhothai (Hein et al. 1986; Thansawangdumrong 2005).

Barbetti and Hein (1989) assessed the development of the ceramic industry of the Ban Ko Noi kiln complex by investigating stratigraphic information including changes in kiln type (from in-ground to above-ground cross draft). The in-ground kilns are believed to be the earlier kiln type used and being constructed by tunneling into a natural hill or riverbank. The above-ground cross draft kilns are believed to be younger as they were mostly built over the ruins of earlier in-ground kilns. Their kiln structures (chimney and chamber) are preserved above the ground surface. Barbetti and Hein (1989) suggest that the change of kiln type happened for maintenance or temperature adjustment reasons. For example, changing the size of the kilns permitted an improved temperature control. Also, it allowed for uncomplicated rebuilds when kilns were made unusable by floods, which represented a constant threat to production sites nearby rivers.

Different dating techniques have been applied to acquire insights into the chronology of ceramic production in northern Thailand. Barbetti and Hein (1989) have used radiocarbon dating for charcoal from several kilns found, for example at Ban Ko Noi and Ban Pa Yang archaeological sites in the Sukhothai area. The results revealed a wide age range for the active production period from between the tenth to the seventeenth century AD (Supplementary Table A). In contrast, TL ages of sherds from the same sites dated earlier by Robertson and Prescott (1988) indicate a later onset of the production period starting in the twelfth and extending into the seventeenth century AD (Supplementary Table B). Bishop et al. (1992) used radiocarbon dating to investigate the link between river terrace erosion and the cessation of the ceramic industry at Ban Ko Noi in the Sukhothai area. They found that the latter occurred around the sixteenth century AD, hence prior to the time of terrace erosion in the eighteenth century AD. Sako (2017) used radiocarbon dating of charcoal samples which were buried with Sukhothai potteries found in the Baray and concluded that these were used during the early fourteenth century AD (Supplementary Table C).

Compared to the Sukhothai area, sites presenting the Lanna ceramic group style within the region of Nan still lack proper chronometric dating. The ceramic production at Ban Bo Suak, in particular, was assumed to have been active around the same time as the Sukhothai kiln sites, for example the Ban Ko Noi kiln complex. This was concluded from

pottery pieces from Ban Ko Noi and Ban Bo Suak found during the Nan ancient city wall excavation (Boonyai 2012; Nokngam 2018). For the Ban Bo Suak archaeological site, it is believed that the majority of ceramic production began around the thirteenth century AD when the area belonged to the Nan Kingdom (Le May 1933). The Nan Kingdom had a close relationship with the Sukhothai Kingdom with regard to religion (Buddhist), arts, politics, and kinship during AD 1356–1442 (Nokngam 2018). Furthermore, Praicharnjit (2011) suggests that the Ban Bo Suak kiln site was called “Ban Tao Hai Jae Liang” in the local Nan historical document. The sound of “Jae Liang” sounds similar to “Chaliang”, a place that was located in the Sukhothai area and produced large amounts of ceramics (Le May 1933). Moreover, it is recorded in the annual of Nan (Pharitdet 1918) that King Intakaen of Nan had been overthrown by his brothers and escaped to “Ban Tao Hai Jae Liang” in AD 1432 before traveling southward to Chaliang city. The link between the king’s history and the village naming suggests that the potters of the Ban Bo Suak kiln site may have originally come from the Sukhothai area. However, there is no detailed study on this migration and further evidence is needed to substantiate these claims (Le May 1933).

The Nan Kingdom was an independent state until AD 1448. After that, Nan became a dependent state of Lanna, which governed the other kingdoms in present-day northern Thailand (Srisum-Ang et al. 1994). The relationship with Sukhothai and Lanna turned Nan into a cultural melting pot which is expressed, for example in the arts. Hence, at the Ban Bo Suak kiln complex, the style of the kilns, ceramics, and imprinted clay tablets (Phra Pim) shares similarities with those from the other sites in Lanna and Sukhothai (Praicharnjit 2011). However, the Ban Bo Suak kiln complex shows a technique in the production, which is different in comparison to sites in Lanna and Sukhothai. In Nan, “saggars” (protective boxes) were used, i.e. earthen boxes with three holes to release heat at the sides and to protect the ceramics from contamination of dust during the production (Supplementary Figure 3). Before being placed into a kiln, ceramics were stored inside saggars. In Eastern Asia, the use of this technique is otherwise only known from China, Vietnam, and Japan during this time (Praicharnjit 2003; Stevenson and Guy 1997; Thansawangdumrong 2005).

From the historical point of view, the ceramic industry at Ban Bo Suak village is assumed to have ended in the early sixteenth century AD after the reign of King Mekut of Lanna due to the first Burmese invasion (Shaw 1981; Thansawangdumrong 2005). However, solid references about the timing of the decline of the ceramic production are lacking. Connecting the decline of ceramic production with the Burmese invasion in AD 1560 is doubtful since there is evidence for subsequent human occupation in the Nan area. In fact, arts from local craftsman, such as Buddha images, were still

produced when Nan was under Burmese rule during AD 1560–1785 (Nokngam 2018), allowing for the assumption that ceramic production was also still active at this time.

Study site

According to Praicharnjit (2011), the area of the Ban Bo Suak kiln complex covered 3–4 km² nearby the Luang (local name: Nam Suak) and Puan (local name: Huay Puan) creeks, both tributaries of the Nan River. Currently, the area of Ban Bo Suak and Ban Nong Tom village is located in the Suak subdistrict (Fig. 2A). The kilns are mainly found buried in the ground and their insides are filled with sediment.

Since 1999, several kilns in Ban Bo Suak village (Fig. 2B) have been excavated during a community-based archaeological project (Praicharnjit 2003). The project was extended in 2007 by the collaboration between the local authorities and the Fine Arts Department of the Ministry of Culture of Thailand to excavate other kilns in the Ban Nong Tom village (Fig. 2A). The present kiln type is identified as an above-ground cross draft kiln single chamber and a clay-slab structure. The latter is produced by adding wet locally found silty clay to the structure and stabilising it by firing. These kilns are constructed with three essential parts: a chimney, a chamber, and a firebox (Fig. 2C). The ceramics found on site are mostly green glazed stoneware such as jars and shallow bowls. These shallow bowls have been decorated with fish imprints which is typical for the Lanna region.

For this study, we collected samples from two sites of the Ja-Manus (JMK) and Nong Tome (NTO) kilns of the Ban Bo Suak kiln complex in May 2019 (Fig. 2A). JMK is located nearby the Luang Creek in the residential area of Mr. Manus Tikham and four kilns have already been excavated in 1999 at this site (Praicharnjit 2011). We collected samples for luminescence dating from kiln JMK1 (Tao Ja-Manus kiln; Fig. 2C) and JMK2 (Tao Chuen kiln). JMK1 is situated on a natural hill with its firebox facing towards the Luang creek. This kiln is 3.0 m wide and 6.5 m long. According to the excavation report, only a small part of the chimney was exposed above the terrain surface. The chamber and firebox collapsed prior to the excavation (Praicharnjit 2011). The chimney comprises two individual layers of loam, possibly related to enforcing the structure after initial construction. Kiln JMK2 is smaller than JMK1, being 1.4 m wide and 4.5 m long. The kiln-mound of JMK2 was well-preserved and its inside was filled with sediment (Praicharnjit 2011). Both JMK1 and JMK2 were buried by sediment with a thickness of ca. 1.7 m measured from the top of present terrain to the floor of kiln firebox. However, they are classified as above-ground cross draft kilns. At the JMK site, many pottery pieces were found both next-to and inside the chambers and also in a pit nearby JMK1 (Fig. 2B). This pottery pit

was presumably used as a repository for defective ceramics (Choopoon 2001). We found many broken pottery pieces and none of them was in good enough shape to identify the specific type. In general, types of pottery found at this site are green glazed plates, bowls, and jars with a single mouth rim decorated with a bird motive. Imprinted clay tablets (Phra Pim) of Sukhothai and Chinese ceramics, presumably of Ming Dynasty age (AD 1368–1644), were previously found on this site (Nokngam 2018). The changes of ceramic style at the JMK site suggest that it was likely operated for 200 years (Choopoon 2001).

The second site (NTO) is located approximately 500 m south of JMK (Fig. 2A). At this site, two kilns were excavated by the Fine Arts Department of the Ministry of Culture of Thailand in 2007. The NTO complex is situated on a natural hill, nearby Puan Creek. We collected samples from one kiln referred to as Tao Nong Tome No. 2 (Boonyai 2007). The kiln (further referred to as NTO) is rather small with 1.7 m in width and 4.7 m in length. All investigated kilns (NTO and JMK) are at a similar terrain elevation. However, the NTO kiln is less deeply buried than those at the JMK site; depth from the present terrain surface to the kiln floor of the firebox is ca. 0.5 m. Due to the small size of the kiln, it is assumed that the potters have opened the ceiling of the chamber after each use (Boonyai 2007). The ceramics found on site were mostly green glazed plates and bowls.

Methods

Sampling

Ceramic samples were collected from the pottery pit nearby JMK1. The pit was originally opened at the same time as JMK1, i.e. during the excavation campaign that took place in October 1999. In the pit, pieces of broken ceramics and of charcoal were found surrounded by homogeneous sediments. The ceramics from this pit are identified to be of the Lanna ceramic group style (Praicharnjit 2011). We hypothesize that this pit is of the same age as the JMK1 kiln, and speculate it was used to dispose ceramics of poor quality or that has been broken during the manufacturing process. According to Malee and Thiansem (2015), the chemical composition of ceramics from Ban Bo Suak shows that they were fired to more than 1000°C until their surface formed mullite grains. For this pit, seven pieces of pottery (JMK-P1 to JMK-P7; Table 1) were collected for luminescence dating and the sediment surrounding the pottery was collected for external dose rate determination. Furthermore, two charcoal samples were taken for radiocarbon dating (BS-P1 and BSP2; Table 2), found at 25 cm depth and mixed in with ceramics pieces in the pit.

Fig. 2 **A** Location of the kiln sites investigated in this study. **B** At the kiln site JMK, samples were collected from two kilns, a pottery pit, and exposed flood sediment. **C** Sketch of an excavated kiln structure (JMK1) and the sample locations within the fire box. The sediment profile and samples collected for OSL are shown in relation to the kiln (satellite images derived from Microsoft Bing 2015)

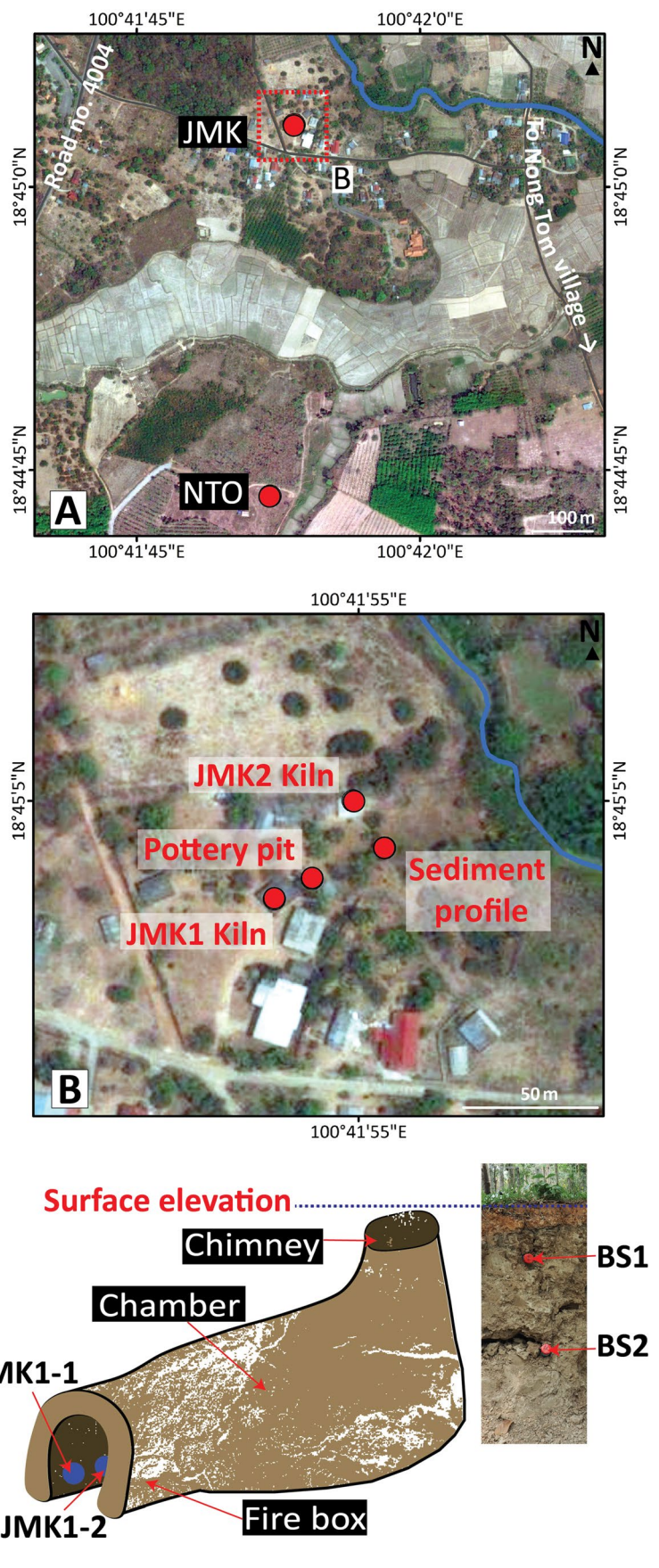


Table 1 Overview of samples for luminescence dating

Sample name	Material	Depth ^b (cm)	Grain size (μm)	Method	Aliquot size ^a
<i>Site: JMK</i>					
JMK-P1	Pottery	30	63–200	TL, OSL	SA
JMK-P2	Pottery	30	63–200	TL, OSL	SA
JMK-P3	Pottery	30	63–200	TL, OSL	SA
JMK-P4	Pottery	30	63–200	TL, OSL	SA
JMK-P5	Pottery	30	63–200	TL, OSL	SA
JMK-P6	Pottery	30	63–200	TL, OSL	SA
JMK-P7	Pottery	30	63–200	TL, OSL	SA
JMK1-1	Kiln	160	105–177	OSL	I, MA, SA
JMK1-2	Kiln	160	105–177	OSL	MA, SA
JMK2-1	Kiln	150	105–177	OSL	MA, SA
JMK2-2	Kiln	150	105–177	OSL	MA, SA
JMK2-3	Kiln	150	105–177	OSL	MA, SA
BS1	Fluvial	30	105–177	OSL	MA, SA
BS2	Fluvial	70	105–177	OSL	MA, SA
BS3	Fluvial	30	105–177	OSL	I, MA, SA
<i>Site: NTO</i>					
NTO1	Kiln	40	105–177	OSL	MA, SA
NTO2	Kiln	40	105–177	OSL	MA, SA
NTO3	Kiln	40	105–177	OSL	MA, SA

^a *I* individual grains (test only), *MA* mini-aliquots; ca. 10–15 grains, *SA* small aliquots; 2 mm stamp with ca. 130 grains (for kiln and fluvial sediment samples) and 6 mm stamp with ca. 1350 grains (for pottery samples)

^b Depth below the terrain surface prior to excavation. Both sites are at the same elevation with ca. 180 m above mean sea level

Table 2 Radiocarbon dating results for two charcoal samples from the pottery pit and for four charcoal samples from the sediment profile. In addition, BBS-1 and BBS-2 are from Praicharnjit (2011) and were obtained for samples from the first excavation in 1999. The

original data has been re-calibrated for this study. Reported ages have been rounded to full decades. *pMC* percent Modern Carbon (post-bomb results)

Sample	Lab code	Depth (cm)	¹⁴ C Age	Calibrated radiocarbon age (AD)	Probability (%)
BSF-T1	Poz-128732	35	118.42 ± 0.34 pMC (R Date -1358 ± 23)	1950–1960	20
				1980–1990	76
BSF-T2	Poz-128733	35	136.49 ± 0.36 pMC (R Date -2499 ± 21)	1950–1960	6
				1970–1980	90
BSF-B1	Poz-128734	65	119.32 ± 0.34 pMC (R Date -1419 ± 23)	1950–1960	20
				1980–1990	75
BSF-B2	Poz-128735	65	121.34 ± 0.38 pMC (R Date -1554 ± 25)	1950–1960	17
				1980–1990	79
BS-P1	Poz-128736	25	115 ± 30 BP	1680–1740	26
				1750–1760	2
				1800–1940	68
BS-P2	Poz-128737	25	65 ± 35 BP	1690–1730	26
				1810–1920	70
BBS-1	Beta-140087	-	670 ± 60 BP	1230–1240	1
				1260–1410	95
BBS-2	Beta-140088	-	450 ± 60 BP	1330–1350	2
				1400–1530	76
				1550–1630	18

Of two kilns, JMK1 and JMK2, the walls of the fire boxes were sampled for luminescence dating (Fig. 2C), expecting that heating during use, i.e. ceramic production, has depleted the luminescence signal in the quartz grains of the kiln wall material. The walls were first cleaned by removing and the outer 5 cm before opaque tubes were pushed horizontally into the material. Samples JMK1-1 and JMK1-2 were collected at the same depth, ca. 160 cm below the terrain surface (burial depth) and about 10 cm apart from each other (Table 1; Fig. 2C). Additional material was taken from the surrounding of the sample tubes for dose rate determination. The sampled material is hard and of orange colour; it resembles burned bricks. Samples JMK2-1, JMK2-2, and JMK2-3 were collected from the kiln inside the fire box wall of JMK2 (Table 1), 15 cm apart from each other and ca. 150 cm below the terrain surface.

At the NTO site, we collected three samples (NTO1 to 3; Table 1). Samples NTO1 and NTO2 were collected about 40 cm below the surface from the inside part of the fire box. Sample NTO3 was collected from the outside of the kiln wall. Further samples were collected from an exposure of sediment that buried the JMK kiln complex (Fig. 2C). The sediment is ca. 100 cm thick and consists of one homogeneous silty sand unit. The sediment is assumed to have been deposited by a flood that presumably stopped the production of ceramics at this site. From the sediment, pieces of charcoal were collected for radiocarbon dating in addition to luminescence samples. Sample BS1 was collected at 30 cm depth for luminescence dating together with two charcoal samples (BSF-T1 and BSF-T2; Table 2) for radiocarbon dating. Luminescence sample BS2 was collected 40 cm below BS1. Two further charcoal samples were obtained at a depth of 65 cm (BSF-B1 and BSF-B2; Table 2). Sample BS3 was taken from the same horizon as sample BS1, but about 20 cm horizontally apart. In total, we collected three samples for luminescence dating and four samples for radiocarbon dating from this profile.

Radiocarbon dating procedures

Sample preparation and measurements via accelerator mass spectrometry (AMS) were conducted at the Poznan Radiocarbon Laboratory (PRL), Poland. The six charcoal samples taken from the pottery pit and the sediment profile (Fig. 2C, Table 2) were cleaned using a standard acid-alkali-acid (AAA) treatment (Mook and Streurman 1983). Samples were rinsed with deionized water, treated with hydrochloric acid (10% HCl) for 30 min and with potassium hydroxide (10% KOH) for 30 min. Afterwards, samples were rinsed with HCl (10%) until the solution became sufficiently transparent and was eventually dried in the oven at 40°C. OxCal 4.4 (Bronk Ramsey et al. 2009) was used to calibrate all ages. For the pre-bomb AMS ages (BS-P1 and BS-P2),

the “INTCAL20” calibration curve (Bronk Ramsey 2017; Reimer et al. 2020) was used while post-bomb (modern) samples (BSF-T1, BSF-T2, BSF-B1 and BSF-B2) were calibrated against “Bomb13 NH1” (Hua et al. 2013).

Luminescence dating procedures

Samples for D_e determination were collected using opaque tubes, subsequently opened and processed under subdued red-light conditions to prevent loss of the natural luminescence signal. For the pottery samples, light-exposed surfaces of about 2 mm thickness were removed from both sides by using a rotary tool grinder. The sample material was then softly ground with mortar and pestle. All samples were wet-sieved (63–200 μm for pottery, 105–177 μm for all other samples) and further processed to extract and purify quartz grains (Wintle 1997). The material was treated with HCl (10%) and subsequently with H_2O_2 (30%) to remove carbonates and organic material, respectively. Heavy minerals were removed using density separation (2.7 g cm^{-3}). Quartz grain rinds were etched using HF (40% for 1 h).

For D_e measurements, grains were mounted onto stainless-steel discs by Freiberg Instruments using silicone oil stamps. Three different aliquot sizes were used: (1) small aliquots (SA) with silicon stamp sizes of 2 mm containing ca. 130 grains (for kiln and fluvial sediment samples) and 6 mm with ca. 1350 grains (for pottery samples; Table 1); (2) individual grain aliquots (I) with only one grain mounted; and (3) mini-aliquots (MA) with 10–15 grains attached to the discs by a spot of silicon oil applied with a pin.

D_e measurements were conducted using an automated Risø reader (TL/OSL-DA-15C/D) updated with a DA-20 controller unit. The reader is equipped with a $^{90}\text{Sr}/^{90}\text{Y}$ beta source delivering ca. 0.11 Gy s^{-1} which was calibrated with the LexCal 2014 quartz standard. For OSL measurements, sample material was stimulated using blue light-emitting diodes (LEDs, $\lambda_{\text{max}} = 470 \text{ nm}$, 34.4 mW cm^{-2}). For TL measurements, the samples were heated by the reader heater plate directly under the photomultiplier tube (heating rate 3°C s^{-1}). The emitted luminescence signals were filtered through a 7.5 mm thick Hoya U-340 UV filter for both approaches. For TL, we also tested the performance using a blue-transmitting filter set (Schott BG-39 and Corning 7-59). OSL measurements were conducted using the single-aliquot regenerative-dose (SAR) protocol (Table 3) following Murray and Wintle (2000). Only for the pottery samples, a hot-bleach step was applied for 60 s at 230°C at the end of every SAR cycles to reduce recuperation (Murray and Wintle, 2003). Sensitivity changes occurring during the course of the SAR protocol were corrected for by applying L_i/T_x ratios, where L_i is the natural (L_n) or regeneration (L_x) dose, and T_x the test dose (1.14 Gy or 1.16 Gy) applied to the aliquot following each L_i measurement (Murray and Wintle

Table 3 SAR protocols used for D_e determination

Method	Step	Protocol
TL	1*	Irradiation; 4.50, 2.25, 6.74, 0, 4.50 Gy
	2 ^a	Preheat of 200 °C for 10 s
	3	Thermal stimulation to 450 °C (L_t)
	4	Irradiation; test dose of 1.14 Gy
	5 ^a	Preheat of 200 °C for 10 s
	6	Thermal stimulation to 450 °C (T_x)
	7	Repeat steps 1–7 with the other regenerative doses during the subsequent cycle
OSL	1*	Irradiation; given regenerative doses are 4.60, 2.32, 6.95, 9.26, 0, 4.60 Gy for JMK1-1 kiln samples 6.95, 3.47, 0, 6.95 Gy for JMK kiln samples 1.14, 0.57, 1.71, 0, 1.14 Gy for JMK pottery samples, with hot-bleach step 5.77, 2.31, 0, 5.77 Gy for NTO kiln samples 5.77, 11.54, 23.08, 0, 5.77 Gy for BS sediment samples
	2	Preheat of 200 °C for 10 s
	3	Infrared stimulated luminescence (IRSL) measurements 40 s at 0 °C
	4 ^b	Optical stimulation for 60 s at 125 °C (L_t)
	5	Irradiation; test dose of 1.16 Gy
	6	Preheat of 200 °C for 10 s
	7	Optical stimulation for 60 s at 125 °C (T_x)
	8 ^c	Optical stimulation for 60 s at 230 °C (hot-bleach step)
	9	Repeat steps 1–7 with the other regenerative doses during the subsequent cycle

*Omitted during the first SAR cycle

^aThis step was excluded for the non-preheat TL measurements

^bOnly conducted for the last cycle of the measurement

^cOnly applied for pottery samples

2000). Preheat plateau, dose recovery, and thermal transfer tests were conducted for OSL measurements on sample JMK1-1 to ensure protocol performance. These tests were done using SA with five different preheat temperatures from 180 to 260 °C in 20 °C steps. Preheats were applied prior to stimulation of L_n , L_x , and T_x doses with a heating rate of 3 °C s⁻¹ and held for 10 s. For both thermal transfer and dose recovery tests (given dose of ca. 4.60 Gy), five aliquots per preheat temperature were LED bleached, measured, and an average D_e value was derived using the Central Age Model (CAM; Galbraith et al. 1999). The preheat plateau test was conducted on the natural signal of 48 aliquots for each temperature. D_e values were determined for all samples by integrating the first 0.4 s of stimulation and subtracting the last 20 s. An exponential curve fitting was used for the dose response curve. The following rejection criteria were applied to OSL D_e measurements: (1) a recycling ratio limit of 10%, (2) a maximum test dose error of 10% for SA and 20% for MA, (3) a maximum recuperation of 10% for SA and of 20% for MA, and (4) T_x signals larger than 3 σ background. Further details on rejection and the number of rejected aliquots are provided in the Table D in the Supporting Information. For the statistical analysis of obtained OSL D_e values, two different age models were applied: the CAM and the

Minimum Age Model (MAM; Galbraith et al. 1999). Details regarding the latter are described below. Age models were calculated using the Luminescence Package for RS studio (Kreutzer et al. 2012). Additional dose recovery tests were conducted on additional kiln (JMK2-3 and NTO2), one fluvial (BS3) and two ceramic samples (JMKP1 and P6).

TL measurements were conducted on seven pottery samples (Table 1) following two variants of the SAR protocol, one without and one with applying preheating to 200 °C for 10 s (Table 3). TL signals were readout between room temperature and 450 °C. A dose recovery test with a given dose of ca. 4.50 Gy was performed on JMK1-1.

For dose rate determination of sedimentary samples, about 290 g of material surrounding the tubes during sampling was collected and dried. The material was then transferred to plastic containers and wrapped air-tight to retain any radon produced. Samples were kept like this for over a month to allow radionuclide concentrations to reach the equilibrium state before measurement (Guibert and Schvoerer 1991). The concentration of dose rate relevant elements (U, Th, K) of the kiln wall material, the fluvial sediment, and the material surrounding the ceramic in the pottery pit were determined by high-resolution gamma spectrometry (HRGS) at the VKTA laboratory (Dresden, Germany). The

dose rate samples were also used to determine field water content. For dose rate calculation, a water content of $5 \pm 3\%$ was assumed to best represent long-term conditions. Dose rates and ages were calculated using ADELE-2017 software (Degering and Degering 2020).

In the case of ceramics, further details for dose rate determination have to be addressed. We hypothesized that a single event filled the pit as we found the infilling sediments to be homogeneous. One component of dose rate will come from the sediments surrounding the ceramics and dose rate determination was conducted as described above for sedimentary samples. The other component comes from the pottery pieces themselves. Hence, we used the outer part of the pottery samples, ground to $<200 \mu\text{m}$, to determine the dose rate by neutron activation analysis (NAA). In contrast to HRGS, NAA requires a much smaller amount of material which in this case was a restricted by the size of the particular samples. NAA analyses were carried out by Bureau Veritas Laboratories, Canada. The final dose rate calculation was done using a layer model in ADELE software, in which the ceramic sample represents one dosimetric layer in the middle. The dosimetric data from the surrounding sediment was used for the top and bottom layer of the middle layer (Table 4).

Results of radiocarbon dating

Results of the six radiocarbon samples are presented in Table 2. For the two samples taken from the pottery pit, radiocarbon ages of 115 ± 30 ^{14}C yr BP (BS-P1) and 65 ± 35 ^{14}C yr BP (BS-P2) were determined which correspond to

a wide age range after calibration, between AD 1680 and AD 1940, with the highest likelihood in the nineteenth (BS-P1) and early twentieth (BS-P2) century AD (68% and 70%, respectively). The ^{14}C measurements of all charcoal fragments from the fluvial sediment indicate modern (post-bomb) ages. These modern ages could either indicate that the fluvial sediment was indeed recently deposited or that the charcoal particles were introduced after sediment deposition. This could, for example, be a result of roots that have grown into the sediment and were later burned, or of insects that buried charcoal particles (e.g. Dickau et al. 2015). The radiocarbon ages are unexpected in the context of the flood deposits and are discussed below together with the age estimates based on luminescence dating.

Luminescence properties and performance

Thermoluminescence signal properties

TL measurements were only tested on pottery samples. There, TL signals of the quartz were expected to show TL peaks at 325°C and/or 375°C (Wintle 1997). However, the samples investigated here hardly emit a natural signal using both the ultra-violet and blue-transmitting filter sets. This is emphasised by comparing the natural signal with the “zero” irradiation signal during the SAR measurement (Fig. 3A, B). The TL glow curves of neither measurement (with and without preheating) presented dominant peaks at 325°C or 375°C . As expected, the non-preheated measurements

Table 4 Results of dosimetric measurements

Sample	wc ^a (%)	K (%)	Th (ppm)	U (ppm)	Dose rate (Gy ka^{-1})
JMK-P1 sed	3.27	0.44 ± 0.05	8.40 ± 0.50	2.70 ± 0.30	-
JMK-P1 pot	-	0.90 ± 0.08	15.90 ± 0.79	3.40 ± 0.27	2.43 ± 0.09^b
JMK-P6 sed	3.27	0.44 ± 0.05	8.40 ± 0.50	2.70 ± 0.30	-
JMK-P6 pot	-	1.10 ± 0.09	16.10 ± 0.81	3.60 ± 0.31	3.17 ± 0.19^b
JMK1-1	2.75	0.52 ± 0.05	9.50 ± 0.60	2.51 ± 0.29	1.86 ± 0.17
JMK1-2	2.75	0.52 ± 0.05	9.50 ± 0.60	2.51 ± 0.29	1.86 ± 0.18
JMK2-1	1.24	0.55 ± 0.05	9.00 ± 0.60	2.40 ± 0.30	1.82 ± 0.14
JMK2-2	1.24	0.55 ± 0.05	9.00 ± 0.60	2.40 ± 0.30	1.82 ± 0.13
JMK2-3	1.24	0.55 ± 0.05	9.00 ± 0.60	2.40 ± 0.30	1.82 ± 0.14
BS1	6.64	0.80 ± 0.06	10.00 ± 0.60	2.90 ± 0.40	2.22 ± 0.19
BS2	7.13	0.81 ± 0.08	10.40 ± 0.60	3.00 ± 0.30	2.25 ± 0.17
BS3	6.64	0.80 ± 0.06	10.00 ± 0.60	2.90 ± 0.40	2.22 ± 0.18
NTO1	2.55	0.37 ± 0.04	9.70 ± 0.60	2.80 ± 0.30	1.84 ± 0.16
NTO2	1.32	0.37 ± 0.03	9.10 ± 0.60	3.00 ± 0.30	1.84 ± 0.13
NTO3	2.55	0.37 ± 0.04	9.70 ± 0.60	2.80 ± 0.30	1.85 ± 0.15

^aWater content as measured in the laboratory. Samples were collected during the dry period (May 2019), to account for higher water contents during monsoon season, a long-term water content of $5 \pm 3\%$ was used for DR determination

^bPottery dose rates were calculated using a layer model with ADELE software

showed a very prominent peak at 125 °C that is known to be unstable (Fig. 3C; cf. Aitken 1985). After laboratory irradiation, the TL emissions are dominated by a peak at 260 °C that is not present in the natural sample (Fig. 3D). Also, dose response curves could not be fitted due to scattering of L_i/T_x values. A large increase in sensitivity was additionally observed for the non-preheated in comparison to the pre-heated measurements. In summary, these particular pottery samples are considered non-suitable for TL dating.

Optically stimulated luminescence signal properties

In this section, we explore the quartz OSL signal of the different materials (pottery, kiln wall, fluvial sediment) investigated in this study. Of the seven ceramic samples, only JMK-P1 and JMK-P6 show a recognisable OSL signal but present unusual OSL decay curves (Fig. 4). Measurements of these samples show rather slow decays compared to typical sedimentary samples and the shape of the decay curves is not identical for the natural and regenerative-dose signals of some aliquots. As we recorded significant recuperation, a hot-bleach step was added to the SAR protocol following Murray and Wintle (2003). The measurement results of sample JMK-P1 and JMK-P6 show acceptable OSL signal characteristics but not a clear dominance of the fast component (Fig. 4). Also, the amount of emitted luminescence was comparatively low. We had to use large aliquots with

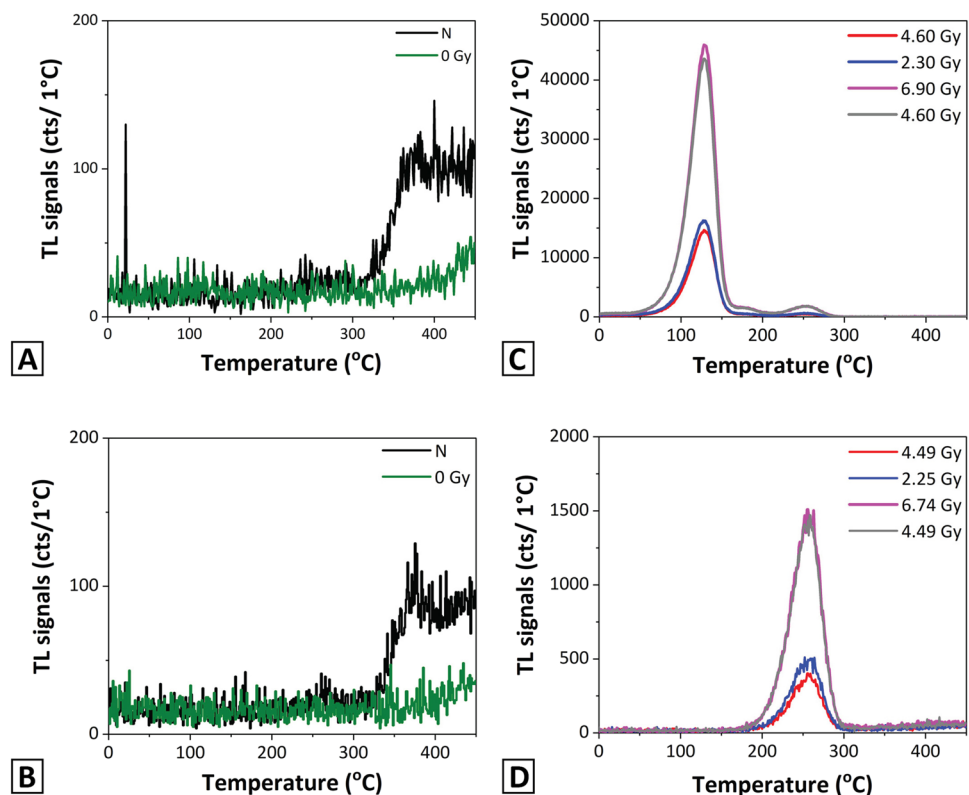
ca. 1350 grains to allow for a bright enough signal to be detected during the measurement (Fig. 4A). Both optical investigation (binocular) and the lack of any response to infrared stimulation prove the absence of feldspar in the samples, which could have explained the shape of the dose response curves.

Considering the unusual shape of the OSL curves of the two suitable samples (JMK-P1, JMK-P6), $D_e(t)$ plots (Fig. 5) were computed to investigate signal stability (Bailey 2000). Ideally, D_e values should remain stable over the stimulation time. The two examples shown in Figure 5 display some variation in the D_e values, which is likely explained by the noisy nature of the OSL signal. There is no clear trend in the values, these scatter around an average value, which implies the presence of stable signals (cf. Steffen et al. 2009).

In contrast to the pottery samples, the kiln and fluvial sediment samples reveal bright OSL signals already for fewer grains (ca. 10% as used for the pottery samples). For D_e determination of those materials, it was originally attempted to measure D_e values for two different aliquot sizes (individual grains (I) and small aliquots (SA)) using JMK1-1 as a test sample. However, none of the individual grain aliquots tested exhibited a measurable OSL signal (Fig. 6A). Therefore, this approach was suspended, and further measurements first concentrated on using SA.

The SA OSL curves show a quick decay during the first 0.4 s (Fig. 6B, D) and dose response curves are well fitted

Fig. 3 Results of TL measurements for sample JMK-P2. **A** and **C** without preheat step, **B** and **D** after preheating at 200 °C. Measurement protocols are presented in Table 3. **A** TL glow curve of a measurement without preheat step reveals a very weak natural TL signal. **B** TL glow curve of a measurement after applying a preheat step show a similarly weak natural TL signal as for A. **C** TL measurements of laboratory given doses. A dominant peak at 125 °C is induced by the artificial radiation. **D** TL measurements after preheating to 200 °C for 10 s. The TL peak at 125 °C is removed and a TL peak at 260 °C becomes most prominent



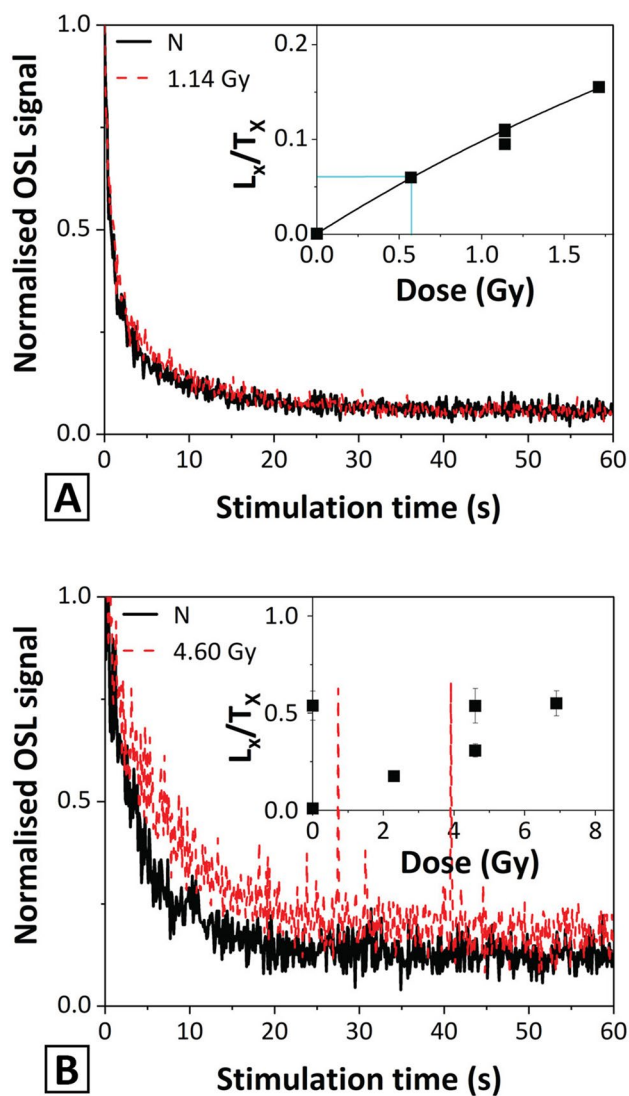


Fig. 4 Exemplary OSL signals and dose response curves of the pottery samples using aliquots with ca. 1350 grains. **A** Example of a good OSL signal for sample JMK-P1 with a hot-bleach step added to the SAR protocol to reduce recuperation. Dose response curves were fitted with a single-saturating exponential function. **B** Example of a poor OSL signal for sample JMK-P7. The dim natural OSL signal shows a different decay shape as the artificial OSL signal (4.60 Gy). The dose response curve fails to fit due to poor recycling

with a single saturating exponential function. While SA measurements present favourable luminescence characteristics, they are prone to suffer from signal averaging when containing partially reset grains. Due to this and the unsuitability of individual grain measurements, mini-aliquots (MA) consisting of about 10–15 grains were produced. While a large number of these aliquots did not pass the rejection criteria, mainly due to test dose errors $>20\%$ and signals below 3σ background (further details in Supplementary Information Table D), a substantial number of aliquots produce acceptable signals (Table 5). The MA signal, although dimer

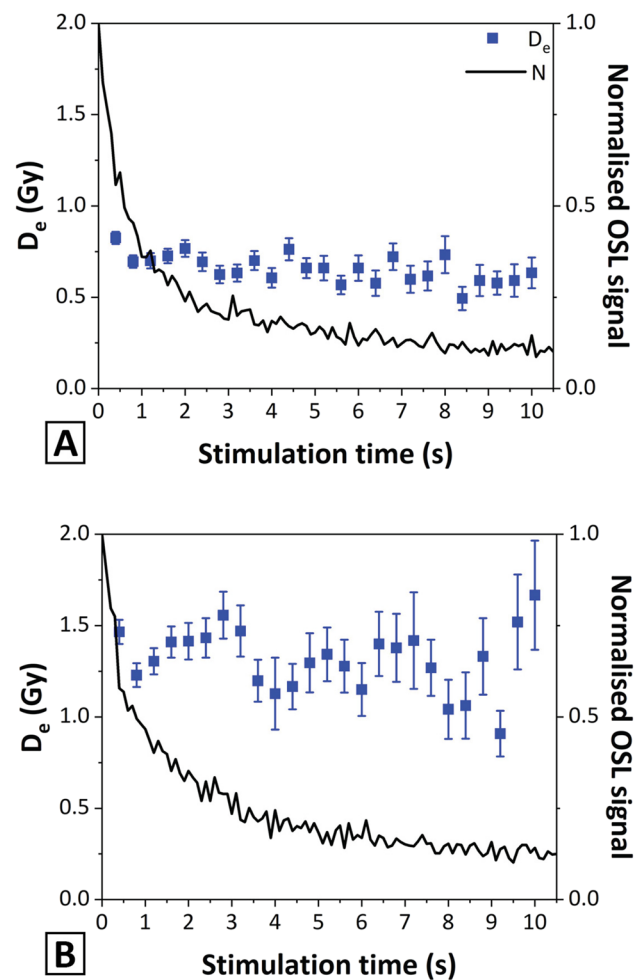


Fig. 5 Natural decay signals and $D_e(t)$ plots of the pottery samples. **A** JMK-P1 and **B** JMK-P6. OSL measurements were both conducted following the SAR protocol adding a $230\text{ }^\circ\text{C}$ hot-bleach step. The OSL signals were normalised to the first value of the decay curve. D_e values were calculated as function of stimulation time over 0.4 s intervals

than those of the SA, shows almost identical properties as the SA (Fig. 6C, E). For both MA and SA, a similar number of D_e values were obtained which are discussed below.

OSL performance tests

The performance of the SAR protocol was tested on SA of sample JMK1-1. To determine the suitable protocol, pre-heat plateau, dose recovery, and thermal transfer tests were conducted and results are presented in Figure 7B. For the preheat plateau test, the natural signal shows a wide scatter of D_e values (48 aliquots) for each of the five preheat temperatures ($180\text{--}260\text{ }^\circ\text{C}$) tested. This likely reflects the effect of partial resetting of the OSL signal in the sample which is unexpected for the heated kiln material. It appears the sample contains a mixture of well-reset and poorly reset

Fig. 6 Exemplary OSL decay signals and dose response curves of the kiln wall sample JMK1-1 (A–C) and fluvial sediment sample BS1 (D–E). **A** Individual grain aliquots (JMK1-1) were tested but measurements were discontinued due to weak natural OSL signals. **B** SA and **C** MA of JMK1-1; the SA aliquots of the kiln walls show a quick decay shape with the signal intensities reaching the residual levels within 0.4 s of stimulation time (dominance of fast component). **D** SA and **E** MA fluvial sediment; the SA and MA OSL signal and decay curve of fluvial sediment show the same behavior as present in kiln walls (**B** and **C**). Dose response curves are fitted well with a single saturating exponential function. The MA have almost identical OSL signal characteristics as SA for both materials but produce generally weaker OSL signals

grains that produce the large scatter and makes it difficult to extract a representative population of D_e values (as discussed further below). For this reason, the preheat plateau test are regarded subsidiary but average D_e values seem to present a plateau starting at 200°C. Since we observe negligible thermal transfer and excellent dose recovery for all preheat temperatures (Fig. 7B), a preheat of 200°C was chosen and applied for all further measurement. Additional dose recovery tests using this temperature setting on two potteries (JMK-P1 and P6), two further kiln (JMK2-3 and NTO2), and one fluvial sample (BS3) all resulted in recovery ratios close to 1.00.

D_e distributions and age models

D_e distributions for all samples are presented in Figure 8 (kiln samples) and Figure 9 (fluvial sediments). All distributions are broad and positively skewed, which is interpreted to be due to differential and incomplete resetting of the OSL signal prior to the event being dated. While this is a common phenomenon in fluvial sediment (cf. Wallinga 2002; Rittenour 2008), we did not expect partial resetting in the heated kiln material. According to Smith et al. (1990), a temperature over 300°C will quickly reset the OSL signal in quartz. While the temperature inside the Ban Bo Suak kilns is not precisely known, Malee and Thiansem (2015) suggest that the ceramics were fired to a temperature of above 1000°C. This leads to the assumption that at least some of the quartz grains obtained from the kiln walls should have been completely reset. Therefore, we interpret D_e values at the lower edge of the distributions as those having been reset completely.

The presence of incompletely reset OSL signals could be explained by the kiln walls having possibly been thicker during ceramic production than after the excavation. The sidewall of the firebox that received most heating during the last time the kiln was operated might have been removed with the burying sediment during excavation. This assumption is supported by the local archaeologists who observed that the kiln walls, for example JMK 1, have two layers at

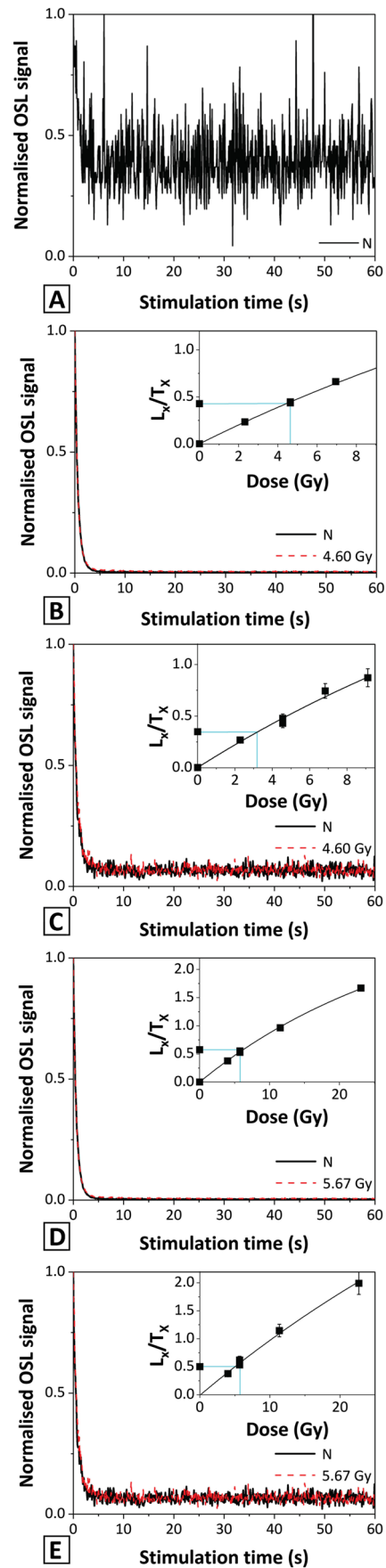


Table 5 Results of D_e determination and ages for all samples obtained by the SA and MA approach. The numbers of individual D_e values (n) used for CAM and MAM calculations (Galbraith et al.

1999) are indicated. Sigma_b values of 0.10 (MA) and 0.20 (SA) were used within the MAM as discussed in the text. The dose rate data for age calculation is given in Table 4

Sample name	Aliquot size	n	OD ^a	CAM		MAM		Age (AD) ^c
				D_e (Gy)	Age (ka)	D_e (Gy)	Age (ka)	
JMK site								
JMK-P1 ^b	SA	10	0.05	0.77 ± 0.02	0.32 ± 0.01	-	-	1690–1720
JMK-P6 ^b	SA	10	0.15	1.33 ± 0.06	0.42 ± 0.02	-	-	1580–1620
JMK1-1	SA	48	0.47	5.77 ± 0.39	3.10 ± 0.24	3.39 ± 0.21	1.82 ± 0.13	-
	MA	44	0.61	4.07 ± 0.39	2.19 ± 0.23	1.82 ± 0.23	0.98 ± 0.13	910–1170
JMK1-2	SA	48	0.53	4.19 ± 0.32	2.26 ± 0.19	1.87 ± 0.15	1.00 ± 0.09	-
	MA	47	0.49	1.63 ± 0.13	0.88 ± 0.08	1.08 ± 0.16	0.58 ± 0.09	1350–1530
JMK2-1	SA	48	0.46	3.75 ± 0.25	2.06 ± 0.16	1.99 ± 0.13	1.09 ± 0.08	-
	MA	44	0.72	2.20 ± 0.25	1.21 ± 0.15	1.37 ± 0.13	0.75 ± 0.08	1190–1350
JMK2-2	SA	48	0.38	3.35 ± 0.19	1.84 ± 0.13	1.95 ± 0.11	1.07 ± 0.07	-
	MA	47	0.71	2.08 ± 0.22	1.14 ± 0.13	1.05 ± 0.16	0.58 ± 0.09	1350–1530
JMK2-3	SA	48	0.38	4.19 ± 0.23	2.30 ± 0.16	2.40 ± 0.15	1.32 ± 0.10	-
	MA	48	0.69	3.11 ± 0.33	1.71 ± 0.14	1.12 ± 0.18	0.61 ± 0.10	1300–1510
BS1	SA	48	0.52	6.12 ± 0.46	2.76 ± 0.24	2.66 ± 0.20	1.20 ± 0.10	-
	MA	35	0.89	4.02 ± 0.62	1.81 ± 0.29	1.28 ± 0.25	0.58 ± 0.12	1330–1560
BS2	SA	48	0.41	4.99 ± 0.30	2.22 ± 0.16	2.65 ± 0.17	1.18 ± 0.09	-
	MA	42	0.79	3.12 ± 0.39	1.39 ± 0.18	0.98 ± 0.17	0.44 ± 0.08	1510–1660
BS3	SA	48	0.47	6.51 ± 0.44	2.94 ± 0.23	3.35 ± 0.24	1.51 ± 0.13	-
	MA	33	0.46	3.75 ± 0.32	1.69 ± 0.16	2.10 ± 0.28	0.95 ± 0.13	940–1200
NTO site								
NTO1	SA	48	0.41	2.77 ± 0.17	1.51 ± 0.11	1.69 ± 0.13	0.92 ± 0.08	-
	MA	48	0.52	1.84 ± 0.15	1.00 ± 0.09	1.20 ± 0.16	0.65 ± 0.09	1280–1460
NTO2	SA	48	0.36	2.73 ± 0.14	1.49 ± 0.10	1.63 ± 0.10	0.89 ± 0.06	-
	MA	52	0.59	2.05 ± 0.18	1.12 ± 0.11	0.94 ± 0.13	0.51 ± 0.07	1430–1580
NTO3	SA	48	0.40	2.52 ± 0.14	1.37 ± 0.09	1.58 ± 0.12	0.86 ± 0.07	-
	MA	44	0.65	1.99 ± 0.21	1.08 ± 0.12	1.18 ± 0.18	0.59 ± 0.07	1370–1500

^aOverdispersion values were calculated using the CAM (Galbraith et al. 1999)^bFor the pottery samples, only the CAM was used as the number of grains on each aliquot (> 1000) prevents the application of the MAM^cAges (AD) were calculated using the MAM D_e values and are given with reference to the year of sampling (AD 2019) except for the pottery samples which were calculated using the CAM

the chimney (Supplementary Figure 3B) and that the glassy coating of the chamber already collapsed (Supplementary Figure 3E). It can be assumed that the kiln was renovated from time to time during operation, so the walls contained several layers. As the kiln was buried and collapsed before the excavation, the glassy coating was not found in its original location. Furthermore, we collected samples by inserting the tube horizontally through the wall and have to consider that we have sampled material that received less heating than those close to the inner part of the kiln wall, i.e. the resetting heat source.

D_e distributions derived for MA and SA show significant differences even though these were determined for the same samples. Generally, the MA D_e distributions are shifted towards lower values. Considering the young age of the

samples, we assume this is related to an averaging effect, i.e. the mixing of OSL signals from several well and poorly reset grains, which will result in masking the true mean D_e value (Duller 2008). This has, for example, been demonstrated for the nineteenth century AD samples from the Rhine River, for which overestimation was in the order of a few centuries (Preusser et al. 2016). This leads us to regard results of the MA measurements as more reliable than those of the SA. However, the results of both approaches will be discussed as the latter is often preferred in dating studies since it has higher OSL signal output.

To calculate average D_e values for each distribution, we used two different age models (CAM and MAM), with results summarised in Table 5. According to Galbraith et al. (1999), application of the CAM is appropriate only

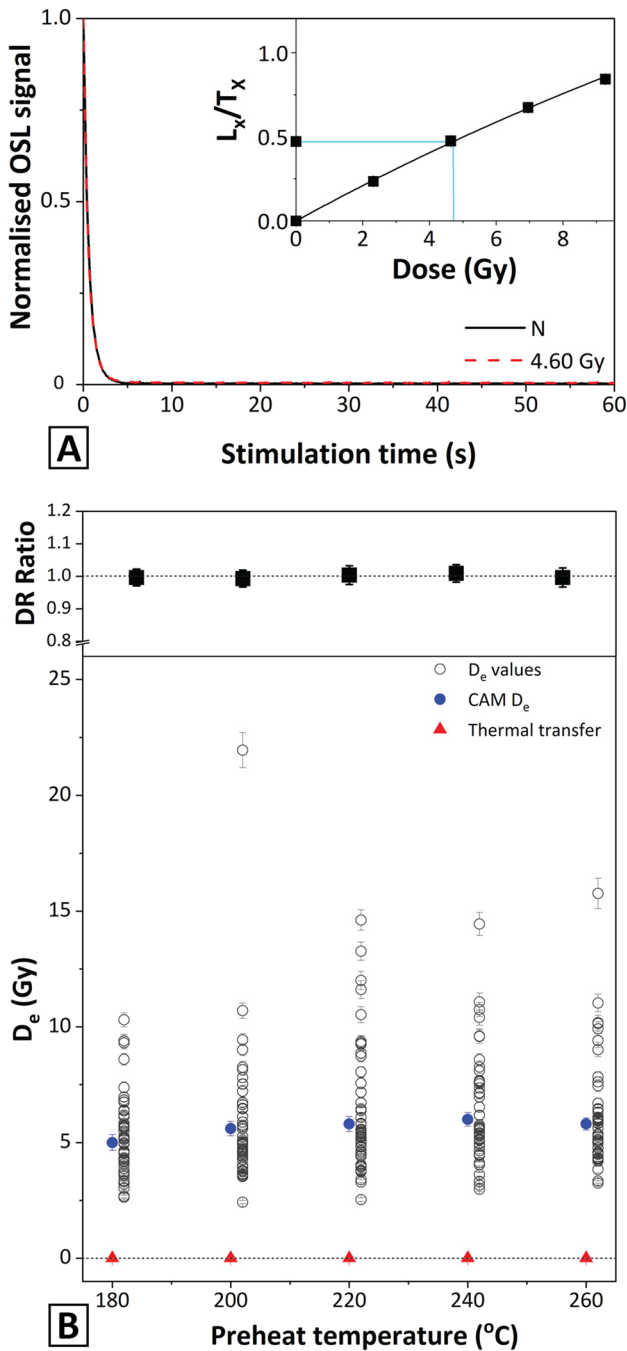


Fig. 7 Results of SAR protocol performance test on JMK1-1 (SA). **A** An example of OSL decay signals and dose response curves of kiln wall sample JMK1-1 using 200 °C preheat for testing the modified SAR protocol. **B** Results of preheat plateau ($n=48$ for each temperature), thermal transfer ($n=5$ for each temperature), and dose recovery (DR) tests ($n=5$ for each temperature) for five different preheat temperatures (180–260 °C). The DR ratio is the measured to given dose ratio. Please note the measurement uncertainties for the first two DR are so small that these are not exceeding the size of the symbol

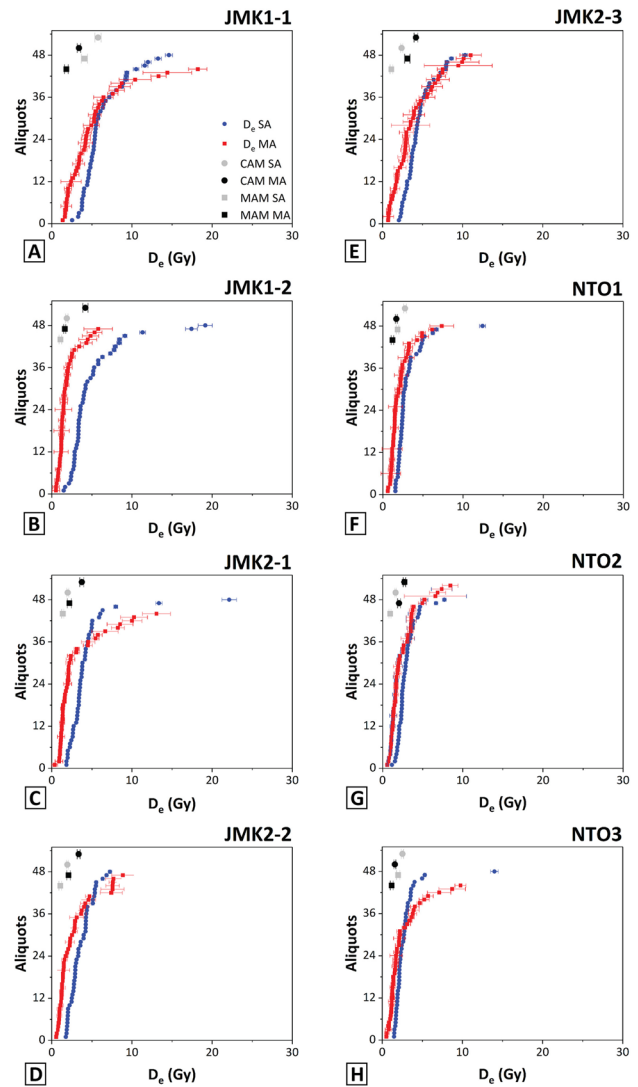


Fig. 8 D_e distributions of the kiln samples for all measurements. Additionally, average D_e values derived using different models (CAM, MAM) are presented

for well-reset samples, which usually have overdispersion (OD) values of 0.10–0.20. Overdispersion describes the presence of greater variability in a data set than would be expected from measurement reproducibility alone. Since the observed OD values obtained in this study (Table 5) are mainly above 0.40 for both kiln and fluvial samples, it is concluded that CAM estimates likely overestimate the real age. However, we are reporting and discussing these values below for completion.

When applying the MAM, it is required to estimate the parameter σ_b , which is the expected overdispersion of the well-reset proportion of the sample. We have computed the effect of σ_b on the average D_e calculation from 0.10 to 0.30 using 0.02 steps (Fig. 10). Notable is that there is only a small impact of σ_b on average D_e values and

Fig. 9 D_e distributions of the kiln samples for all measurements. Additionally, average D_e values derived using different models (CAM, MAM) are presented

based on this we used 0.20 for MA and 0.10 for SA as rather conservative estimates. The larger number of grains on SA is expected to produce some averaging effects and reduces the expected overdispersion (Cunningham et al. 2011).

Figure 11A illustrates the comparison of average D_e values computed using the different age models. As expected, these are systematically higher for CAM. For SA, CAM D_e values range from 2.52 ± 0.14 to 6.51 ± 0.44 Gy and for MA CAM D_e values of between 1.63 ± 0.13 and 4.07 ± 0.39 Gy were obtained. MAM D_e values determined for the kiln samples range between 0.86 ± 0.07 and 1.82 ± 0.13 Gy (SA) and between 0.51 ± 0.07 and 0.98 ± 0.13 Gy (MA; Fig. 11B). For the fluvial sediments, the range falls between 1.18 ± 0.09 and 1.51 ± 0.13 Gy (SA) and 0.51 ± 0.07 to 0.98 ± 0.13 Gy (MA). These observations indicate that the use of 2 mm aliquot size (SA) leads to a significant overestimation of the average D_e likely due to partial resetting of the OSL signal, in particular for young samples (cf. Preusser et al. 2016). Therefore, aliquots with fewer grains are expected to represent the D_e values close to the “true dose” (Li 1994). In combination with the application of MA, with likely few if not only one a single grain contributing to the OSL signal, applying the MAM is the approach of choice to isolate the D_e values that represent the dose absorbed since burial.

Chronological implications

In the following, the dating results for ceramics from the pottery pit, the kiln wall material, and the fluvial sediment are discussed separately before being compared. In the context of this study, it is important to note that radiocarbon and OSL are not determining the age of the same event. With radiocarbon dating, the end of ^{14}C absorption from the atmosphere by organic material is determined, in the present case the death of plants that were later transformed into charcoal. With OSL, the event dated is the resetting of the signal, in the present case the firing of ceramics, the last heating of the kilns, or the last daylight exposure during fluvial transport. However, from the sampling context, it was originally assumed that these events should all be temporally related to the manufacturing process, thus synchronous within the given dating uncertainties. Figure 12 shows the calibrated radiocarbon and OSL ages expressed on the same scale in years (AD) and rounded to full decades. Radiocarbon ages are presented with two-sigma confidence intervals (95.4% probability) and plotted as horizontal lines to display the ages and their uncertainties. For radiocarbon dating, plateaus in the calibration curve produce rather large areas

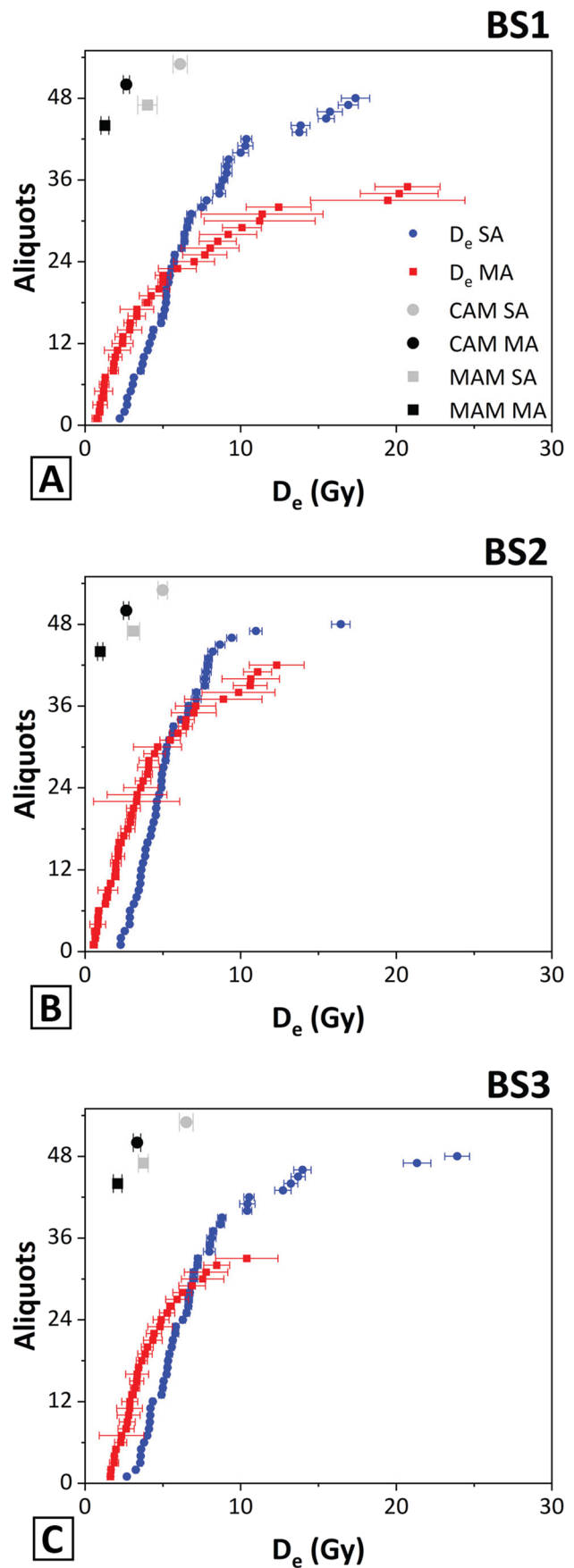
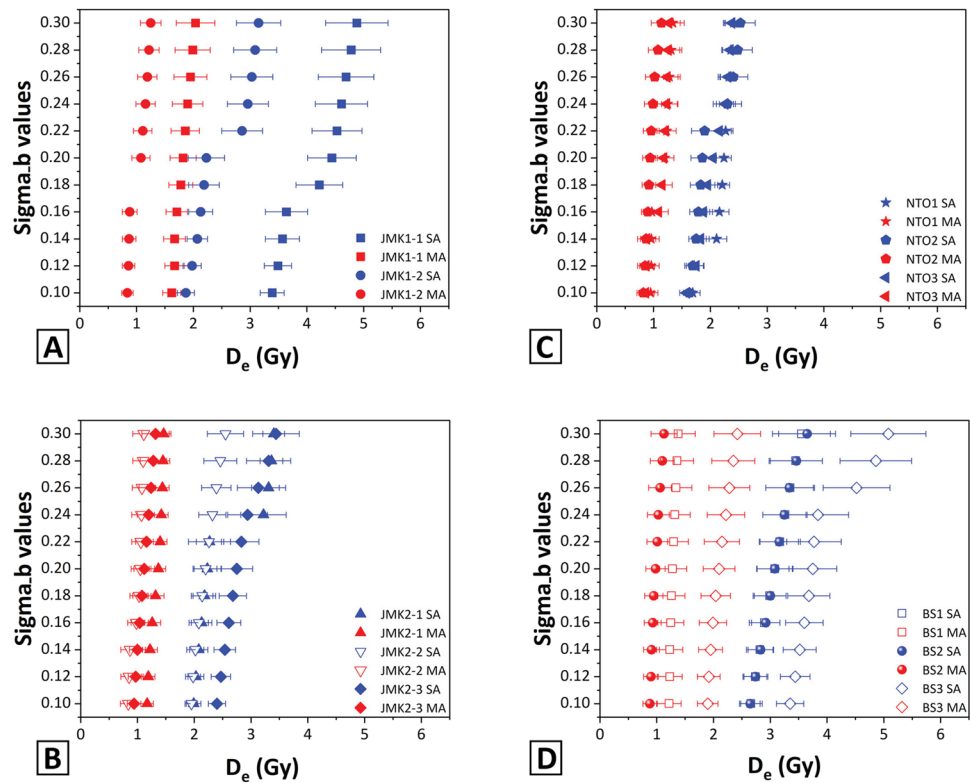


Fig. 10 Sigma_b versus MAM D_e values for all samples. Different sigma_b values indicate only a slightly change of average D_e values for both aliquot sizes (SA and MA) for most of the samples



of possible calibrated ages with different individual likelihoods. For example, for sample BS-P2, the radiocarbon age of 65 ± 35 BP corresponds after calibration to potential time periods with different likelihood: AD 1690–1730 (26%) and 1810–1920 (70%). However, a lower likelihood still requires to fully consider this result, which makes the interpretation of data quite complex.

For the pottery from the JMK site, two OSL ages of AD 1690–1720 (0.32 ± 0.01 ka; JMK-P1) and AD 1580–1620 (0.42 ± 0.02 ka; JMK-P6) were obtained. While the ages do not overlap within the reported error margins, the sampling context strongly implies these should be of the same age. Presumably, this could be explained by uncertainties related to dosimetry, as the setting is rather complex, representing a mixture of sand and ceramic pieces with significant differences in the amounts of radioactive elements. Resolving this problem would have required a detailed description of the site, multiple sampling of layers and objects, and applying complex dose rate models (cf. Guérin, 2015).

The two radiocarbon samples from the pottery pit (Table 2) have very large uncertainties after calibration, with the most likely age in the nineteenth to twentieth century AD (BS-P1: AD 1800–1940 at 68% likelihood; BS-P1: AD 1810–1920 at 70% likelihood). However, calibration of both samples also results in statistically less likely (26%) ages of AD 1680–1740 (BS-P1) and AD 1690–1730 (BS-P2). These ages are in perfect agreement with the OSL age determined

for sample JMK-P1 (AD 1690–1720). Hence, considering all available data, the dated ceramic pieces were likely produced during the late seventeenth or early eighteenth century AD.

The samples from kilns of the JMK site have mainly overlapping OSL ages (JMK1-2: AD 1350–1530; JMK21: AD 1190–1350; JMK2-2: AD 1350–1530; JMK2-3: AD 1300–1510), except for sample JMK1-1 that has a much older age (AD 910–1170). For the samples of the NTO kiln, three OSL ages consistent with each other have been determined (NTO1: AD 1280–1460; NTO2: 1430–1580; NTO3: 1370–1500). This age estimate is corroborated by the previously published radiocarbon ages of AD 1260–1410 (95% likelihood; BBS-1), AD 1400–1530 (76%) and AD 1550–1630 (18%; both BBS-1). In summary, the available data points with exception of JMK1-1 towards a last use of the kilns during the fifteenth century (Fig. 12).

The three OSL ages of fluvial sediments indicate deposition at AD 1330–1560 (BS1), AD 1510–1660 (BS2), and AD 940–1200 (BS3). Please note that BS3 was taken parallel to sample BS1 and is expected to be of the same age. Rejecting this age as an outlier implies deposition between AD 1420–1520 for the fluvial sediments, i.e. most likely during the fifteenth century AD. In contrast, all radiocarbon ages taken from the fluvial sediments have post-bomb ages, i.e. the organic material formed during the second half of the twentieth century. As local witnesses confirmed that the kilns were buried at this time, the radiocarbon ages are

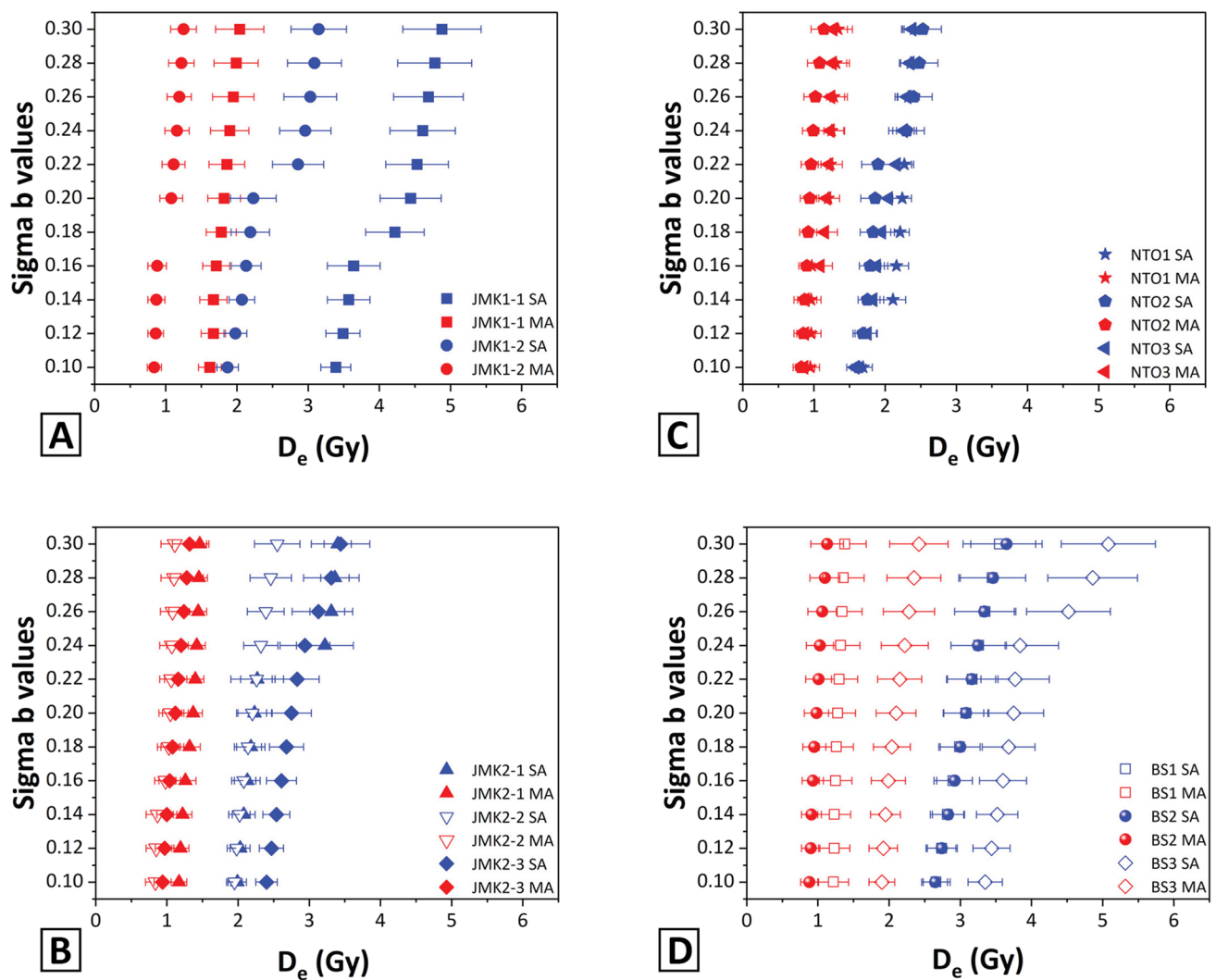


Fig. 11 Comparing average D_e values of kiln and fluvial samples calculated using CAM and MAM for different aliquot sizes. **A** The D_e values calculated with the CAM are generally and significantly higher

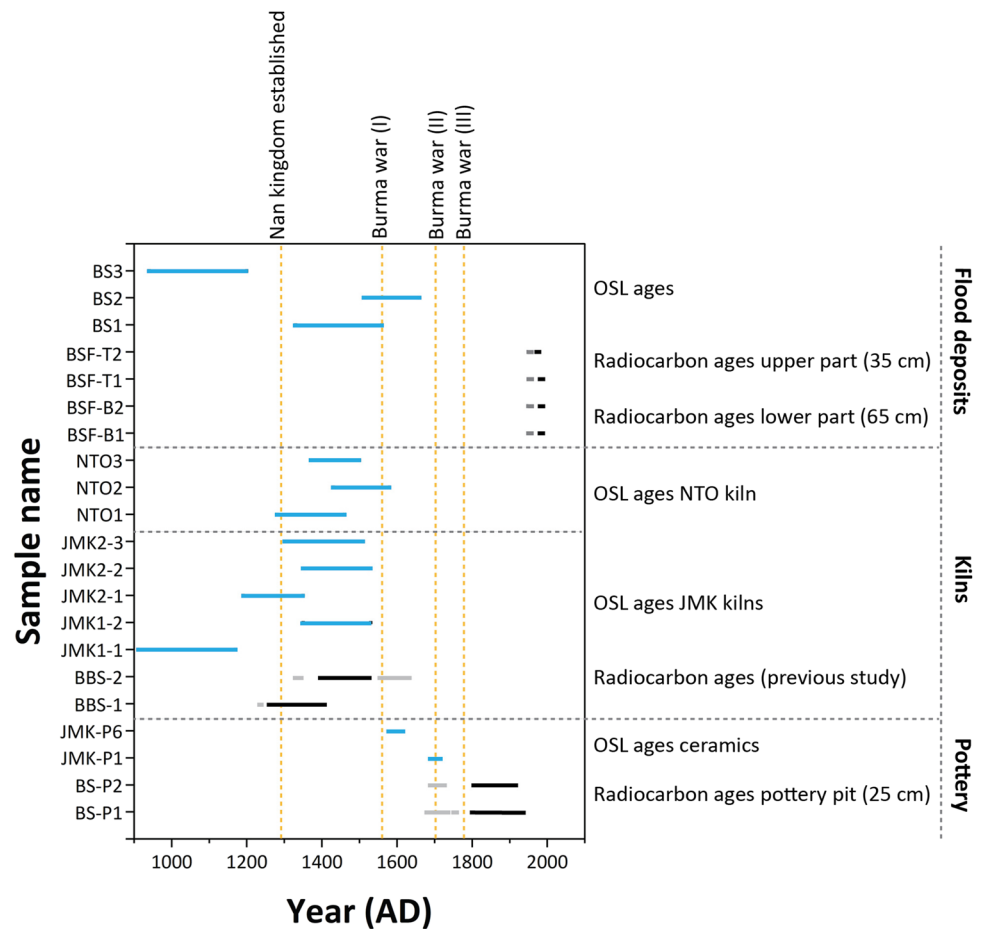
than with the MAM. **B** The D_e values calculated for SA are generally significantly higher than for MA (The red line indicates 1:1 ratio)

likely not related to the flooding event. We speculate that the presence of the organic material in the sediment is likely related to burrowing insects or by roots, an issue that has been reported in the literature for sites from similar settings (Grave and Kealhofer 1999; Tribolo et al. 2010).

While the dating attempts presented proved much more challenging than originally expected, it appears nonetheless eligible to discuss them in terms of historical interpretation. First, the ages reported imply that the last use of the kilns at both sites and the deposition age of the covering fluvial sediment fall into the fifteenth century AD. While the dating uncertainties do not allow to prove a strict relationship on a temporal basis, it seems reasonable to draw a connection between the two events. However, the age of the pottery found in pit nearby the kilns is some 200 years younger. Hence, while the flood may have caused the abandonment

of the now buried kiln, the production of ceramics continued afterwards for quite some time. This observation is in agreement with the data published by Robertson and Prescott (1988) who report ceramic production until the seventeenth century AD in the Sukhothai area. However, it is uncertain where the kiln related to their production phase could have been situated. The fact that the ceramics were disposed implies a certain proximity, but no traces of kilns have been reported above ground surface around the site. Already Shaw (1984) observed this fact and assumed that kilns above ground were destroyed by later agricultural activity. In this context, it should be noted that several rebellions by the local population occurred during 200 years of the Burmese occupation (AD1560–1785). During that time, the current region of northern Thailand and especially Chiang Mai, which was a center of the Lanna Kingdom, was control by Burma as

Fig. 12 Summary of ages derived from radiocarbon (high likelihood = black lines; low likelihood = grey lines) and luminescence (blue lines) dating. The dating of pottery and related charcoal indicates a production of ceramics until ca. AD 1700. On the other hand, the last use of the kilns and the deposition of fluvial sediments burring those occurred around the fifteenth century AD



was the rest of the Lanna state. After one such unsuccessful attempt for liberation, known as the second Burma War in the region, the city of Nan was abandoned for five years (AD 1703–1708). The same happened in AD 1778 (third Burma War), when the inhabitants of Nan city were forced to migrate to Chiengsaen (Pharitdet 1918; Thansawangdumrong 2005), contemporary the north most part of Thailand but under Burmese rule at that time. The city of Nan was only repopulated in AD 1800 when the region was under the rule of the Siam Empire. Hence, a connection of the decline of Lanna ceramic group production with the political situation appears as a more likely explanation.

Conclusions

This study experienced unexpected challenges when aiming at dating the decline of ceramic production at the Ban Bo Suak site in the Nan region, northern Thailand. In contrast to many other regions, quartz grains extracted from ceramic sherds did not show suitable TL signal; only for two out of seven samples, the OSL signal was bright enough to be used for dating purposes. The results for these two samples are

quite scattered, which might be related to dosimetric issues. However, in combination with previously published radiocarbon ages, it appears that ceramic production continued at the site until around AD 1700. All samples taken from the kiln walls show clear evidence for partial resetting of the OSL signal. This is in contrast to previous studies and it is speculated that the heat flux was not high enough in the present setting. The use of too many grains on the aliquots will mask the spread of individual D_e values and averaging effects can lead to significant age overestimation for the samples under consideration. Despite one outlier, the dating results point towards a last use of the kilns during the fifteenth century AD. This coincides with two out of three OSL ages determined for the sediment covering the kilns. Charcoal extracted from the sediment is dated to the second half of the twentieth century (post-bomb) and is likely related to burrowing by insects or roots. This again highlights the need to carefully consider if radiocarbon dating does necessarily reflect the age of the event to be dated. Overall, this study demonstrates the need to carefully consider the methodological challenges that are related to rather well-established physical dating approaches. Despite these limitations, the presented data strongly implies that while a severe flooding

event in the fifteenth century AD buried the kiln sites, this did not stop the production of Lanna group ceramics in the Nan region, which continued for some two centuries.

Supplementary Information The online version contains supplementary material available at <https://doi.org/10.1007/s12520-022-01618-y>.

Acknowledgements We thank your collaborators of the Department of Geology, Faculty of Science, Chulalongkorn University and the Fine Arts Department of Thailand (Local Office No. 7) for supporting the fieldwork as well as for providing samples and data. We would like to thank Mr. Manus Tikham, the owner of the JMK site, for support. We also thank Dr. Peerasit Surakiatchai and Pranot Rattana for supporting the sampling. Furthermore, we would like to thank Dr. Claire Rambeau and Alexander Fülling for guidance and assistance regarding sample preparation. The manuscript was improved following the recommendation by two anonymous referees whom we like to thank.

Funding Open Access funding enabled and organized by Projekt DEAL. This research is funded by the German Science Foundation through grant PR 957/5–1. P. Srisunthon received a grant by the German Academic Exchange Service.

Declarations

Conflict of Interest The authors declare no competing interests.

Open Access This article is licensed under a Creative Commons Attribution 4.0 International License, which permits use, sharing, adaptation, distribution and reproduction in any medium or format, as long as you give appropriate credit to the original author(s) and the source, provide a link to the Creative Commons licence, and indicate if changes were made. The images or other third party material in this article are included in the article's Creative Commons licence, unless indicated otherwise in a credit line to the material. If material is not included in the article's Creative Commons licence and your intended use is not permitted by statutory regulation or exceeds the permitted use, you will need to obtain permission directly from the copyright holder. To view a copy of this licence, visit <http://creativecommons.org/licenses/by/4.0/>.

References

- Aitken MJ (1985) Thermoluminescence dating. Academic Press, London
- Aitken MJ (1998) Introduction to optical dating: the dating of Quaternary sediments by the use of photon-stimulated luminescence. Clarendon Press, Oxford
- Aitken MJ, Tite MS, Reid J (1964) Thermoluminescent dating of ancient ceramics. *Nature* 202:1032–1033
- Bailey RM (2000) The interpretation of quartz optically stimulated luminescence equivalent dose versus time plots. *Radiat Measur* 32:129–140
- Barbetti M, Hein D (1989) Palaeomagnetism and high-resolution dating of ceramic kilns in Thailand: a progress report. *Wld Archaeol* 21:51–70. <https://doi.org/10.1080/00438243.1989.9980090>
- Bó DM, Bernardin AM, Hotza D (2014) Formulation of ceramic engobes with recycled glass using mixture design. *J Cleaner Prod* 69:243–249. <https://doi.org/10.1016/j.jclepro.2014.01.088>
- Boomgaard P (2007) Southeast Asia: an environmental history. ABC-CLIO, California
- Boonyai S (2007) Ban Nong Tome and Ancient Kilns (in Thai). Fine Art Department, Nan Local Office, Nan
- Boonyai S (2008) Report from survey of pre-historical archeological sites in Wiang Sa and Na Noi, Nan Thailand (in Thai). Fine Art Department of Thailand, Chiang mai
- Boonyai S (2012) Report from Nan Ancient City Wall Excavation in Wat Phraya Wat Area by Fine Art Department Local no 7 (in Thai). Ploy Kan Pim, Chiang Mai
- Bronk Ramsey C (2008) Radiocarbon dating: revolutions in understanding. *Archaeometry* 50:249–275. <https://doi.org/10.1111/j.1475-4754.2008.00394.x>
- Bronk Ramsey C (2017) Methods for Summarizing Radiocarbon Datasets. *Radiocarb* 59:1809–1833. <https://doi.org/10.1017/RDC.2017.108>
- Bronk Ramsey C, Higham T, Brock F, Baker D, Ditchfield P (2009) Radiocarbon dates from the Oxford AMS system: archaeometry datelist 33. *Archaeometry* 51:323–349. <https://doi.org/10.1111/j.1475-4754.2008.00457.x>
- Casanova E, Knowles TD, Ford C, Cramp LJ, Sharples N, Evershed RP (2020) Compound-specific radiocarbon, stable carbon isotope and biomarker analysis of mixed marine/terrestrial lipids preserved in archaeological pottery vessels. *Radiocarb* 62:1679–1697. <https://doi.org/10.1017/RDC.2020.11>
- Brown R (1988) The ceramics of South-East Asia: their dating and identification. Oxford University Press, Singapore
- Cheewinsiriwat P (2013) The use of GIS in exploring settlement patterns of the ethnic groups in Nan, Thailand. *Asian Ethnicity* 14:490–504. <https://doi.org/10.1080/14631369.2013.764053>
- Chairat K (2009) Transformation of urban structure and physical elements of Nan City (in Thai). Dissertation Chulalongkorn University
- Choopeen A (2001) The study of kiln and ceramic pattern at Nan Kiln Complex, Ban Bo Suak Nan Thailand (in Thai). Dissertation, Silpakorn University
- Cunningham AC, Wallinga J, Minderhoud PS (2011) Expectations of scatter in equivalent-dose distributions when using multi-grain aliquots for OSL dating. *Geochronometria* 38:424–431. <https://doi.org/10.2478/s13386-011-0048-z>
- Degering D, Degering A (2020) Change is the only constant-time-dependent dose rates in luminescence dating. *Quaternary Geochronol* 58:101074. <https://doi.org/10.1016/j.quageo.2020.101074>
- Dickau R, Aceituno FJ, Loaiza N, López C, Cano M, Herrera L, Restrepo C, Ranere AJ (2015) Radiocarbon chronology of terminal Pleistocene to middle Holocene human occupation in the Middle Cauca Valley, Colombia *Quaternary Int* 363:43–54. <https://doi.org/10.1016/j.quaint.2014.12.025>
- Duller GA (2008) Single-grain optical dating of Quaternary sediments: why aliquot size matters in luminescence dating. *Boreas* 37:589–612. <https://doi.org/10.1111/j.1502-3885.2008.00051.x>
- Galbraith RF, Roberts RG, Laslett GM, Yoshida H, Olley JM (1999) Optical dating of single and multiple grains of quartz from Jimmim rock shelter, northern Australia: Part I, experimental design and statistical models. *Archaeometry* 41:339–364. <https://doi.org/10.1111/j.1475-4754.1999.tb00987.x>
- Gorman CF (1970) Excavations at spirit cave, North Thailand: some interim interpretations. *Asian Persp* 13:79–107
- Graham W (1922) Pottery in Siam. *J Siam Soc* 16:1–27
- Grave P, Barbetti M, Hotchkis M, Bird R (2000) The stoneware kilns of Sisatchanalai and Early Modern Thailand. *J Field Archaeol* 27:169–182. <https://doi.org/10.1179/jfa.2000.27.2.169>
- Grave PR (1995) The shift to commodity: a study of ceramic production and upland-lowland interaction in northwestern Thailand 1000–1650 AD. Dissertation University of Sydney
- Grave P, Kealhofer L (1999) Assessing bioturbation in archaeological sediments using soil morphology and phytolith analysis. *J Archaeol Sci* 26:1239–1248. <https://doi.org/10.1006/jasc.1998.0363>

- Guérin G (2015) Innovative dose rate determinations for luminescence dating. *Elements* 14:15–20. <https://doi.org/10.2138/gselements.14.1.15>
- Guibert P, Schvoerer M (1991) TL dating: low background gamma spectrometry as a tool for the determination of the annual dose. *Int J Radiat Applications and Instrum Part D. Nucl Tracks Radiat Meas* 18:231–238. [https://doi.org/10.1016/1359-0189\(91\)90117-Z](https://doi.org/10.1016/1359-0189(91)90117-Z)
- Hein D, Burns P, Richards D (1986) An alternative view of the origins of ceramic production at Si Satchanalai and Sukhothai, Central Northern Thailand. *SPAFA Digest* 7:22–33
- Hein D, Hill G, Ramsay WRH (2004) Raw or pre-fired: kiln construction at Sawankhalok, North Central Thailand, as a guide to ceramic history. *Int J Hist Archaeol* 8:247–266. <https://doi.org/10.1007/s10761-004-2607-y>
- Hein D (2008) Ceramic kiln lineages in Mainland Southeast Asia. *Ceramics in Mainland Southeast Asia: Collections in the Freer Gallery of Art and Arthur M. Sackler Gallery*. Smithsonian Institution Washington, DC
- Higham C (1989) *The archaeology of mainland Southeast Asia: from 10,000 BC to the fall of Angkor*. Cambridge University Press, Cambridge
- Higham CF, Rispoli F (2014) The Mun Valley and Central Thailand in prehistory: integrating two cultural sequences. *Open Archaeol* 1:2–28. <https://doi.org/10.2478/opar-2014-0002>
- Hua Q, Barbetti M, Rakowski AZ (2013) Atmospheric radiocarbon for the period 1950–2010. *Radiocarb* 55:2059–2072. https://doi.org/10.2458/azu_js_rc.v55i2.16177
- Huntley DJ, Godfrey-Smith DI, Thewalt MLW (1985) Optical dating of sediments. *Nature* 313:105–107. <https://doi.org/10.1038/313105a0>
- Kreutzer S, Schmidt C, Fuchs MC, Dietze M, Fischer M, Fuchs M (2012) Introducing an R package for luminescence dating analysis. *Ancient TL* 30:1–8. <https://doi.org/10.013/epic.44194.d001>
- Lampert CD, Glover IC, Hedges R, Heron CP, Higham T, Stern B, Shoocongdej R, Thompson GB (2003) Dating resin coating on pottery: the Spirit Cave early ceramic dates revised. *Antiquity* 77:126–133. <https://doi.org/10.1017/S0003598X0006141X>
- Le May R (1933) The ceramic wares of North-Central Siam-I. *Burlington Magazine for Connoisseurs* 63:156–166
- Lechterbeck J, Edinborough K, Kerig T, Fyfe R, Roberts N, Shenan S (2014) Is Neolithic land use correlated with demography? An evaluation of pollen-derived land cover and radiocarbon-inferred demographic change from Central Europe. *The Holocene* 24:1297–1307. <https://doi.org/10.1177/0959683614540952>
- Li SH (1994) Optical dating: insufficiently bleached sediments. *Radiat Measur* 23:563–567. [https://doi.org/10.1016/1350-4487\(94\)90100-7](https://doi.org/10.1016/1350-4487(94)90100-7)
- Liritzis I, Singhvi AK, Feathers JK, Wagner GA, Kadereit A, Zacharias N, Li S-H (2013) Luminescence dating in archaeology, anthropology, and geoarchaeology: an overview. Springer, Heidelberg
- Low CA (2004) Sawankoloke-Sukhothai Wares from the Empress Place Site. *Singapore the Herit J* 1:21–37
- Malee U, Thiansem S (2015) Preparation and characterization of clays from different areas in Ban Bo Suak, Nan province, Thailand. *Key Eng Mater* 659:127–131. <https://doi.org/10.4028/www.scientific.net/KEM.659.127>
- Microsoft Bing (2015) Available online: <https://www.bing.com/maps/aerial> (accessed on 6 January 2021).
- Bishop P, Hein D, Maloney B, Fried A (1992) Riverbank erosion and the decline of the Sisatchanalai ceramics industry of north central Thailand. *The Holocene* 2:159–163. <https://doi.org/10.1177/095968369200200207>
- Miksic JN (2006) Chinese Ceramics and the Economics of Early Southeast Asian Urbanisation, 14th to 16th Centuries. *Bull Indo-Pacific Prehist Assoc* 26:147–153. <https://doi.org/10.7152/bippa.v26i0.12004>
- Mook WG, Streurman HJ (1983) Physical and chemical aspects of radiocarbon dating. In *Proceedings of the First International Symposium 14 C and Archaeology*, Groningen, 1981
- Murray AS, Wintle AG (2000) Luminescence dating of quartz using an improved single-aliquot regenerative-dose protocol. *Radiat Measur* 32:57–73. [https://doi.org/10.1016/S1350-4487\(99\)00253-X](https://doi.org/10.1016/S1350-4487(99)00253-X)
- Murray AS, Wintle AG (2003) The single aliquot regenerative dose protocol: potential for improvements in reliability. *Radiat Measur* 37:377–381. [https://doi.org/10.1016/S1350-4487\(03\)00053-2](https://doi.org/10.1016/S1350-4487(03)00053-2)
- Ng S, Wood SH, Ziegler AD (2015) Ancient floods, modern hazards: the Ping River, paleofloods and the 'lost city' of Wiang Kum Kam. *Nat Hazards* 75:2247–2263. <https://doi.org/10.1007/s11069-014-1426-7>
- Nokngam A (2018) A relationship between Nan Sukhothai and Lanna in 14th - 17th century from archaeological evidence. Dissertation, Silpakorn University
- Pharitdet S (1918) *Historical Annals (Pongsawadan Muang Nan) Vol 10 by Phra Chao Suriyaphong Pharitdet (in Thai)*. Samosorn, Nan
- Praicharnjit S (2003) *Community archaeology: past management and community development (in Thai)*. Thammasat University Press, Pathum Thani
- Praicharnjit S (2011) *Archaeology of ceramics in Lān Nā*. Silpakorn University Press, Bangkok, Northern Siam
- Preusser F, Degering D, Fuchs M, Hilgers A, Kadereit A, Klasen N, Krbetschek M, Richter D, Spencer JQ (2008) Luminescence dating: basics, methods and applications. *E&G Quaternary Sci J* 57:95–149. <https://doi.org/10.3285/eg.57.1-2.5>
- Preusser F, May J-H, Eschbach D, Trauerstein M, Schmitt L (2016) Infrared stimulated luminescence dating of 19th century fluvial deposits from the upper Rhine River. *Geochronometria* 43:131–142. <https://doi.org/10.1515/geochr-2015-0045>
- Rajanubhab DSKP, Crosby J (1919) Siamese history prior to the founding of Ayudhdhaya. *Journal of the Siam Soc* 13:1–66
- Reimer PJ, Austin WE, Bard E, Bayliss A, Blackwell PG, Ramsey CB, Butzin M, Cheng H, Edwards RL, Friedrich M (2020) The IntCal20 Northern Hemisphere radiocarbon age calibration curve (0–55 cal kBP). *Radiocarb* 62:725–757. <https://doi.org/10.1017/RDC.2020.41>
- Reynolds TE (1992) Excavations at Banyan Valley Cave, Northern Thailand: a report on the 1972 season. *Asian Persp* 31:77–97
- Rittenour TM (2008) Luminescence dating of fluvial deposits: applications to geomorphic, palaeoseismic and archaeological research. *Boreas* 37:613–635. <https://doi.org/10.1111/j.1502-3885.2008.00056.x>
- Roberts RG, Jacobs Z, Li B, Jankowski NR, Cunningham AC, Rosenfeld AB (2015) Optical dating in archaeology: thirty years in retrospect and grand challenges for the future. *J Archaeol Sci* 56:41–60. <https://doi.org/10.1016/j.jas.2015.02.028>
- Robertson G, Prescott J (1988) The Thai ceramics archaeological project: TL characteristics of the artifacts. *International Journal of Radiat Applications and Instrum. Part D. Nucl Tracks Radiat Meas* 14:299–305. [https://doi.org/10.1016/1359-0189\(88\)90080-5](https://doi.org/10.1016/1359-0189(88)90080-5)
- Sako T (2017) Interpretation of AMS dating by the University of Waikato radiocarbon dating laboratory on charcoal samples from the 2016 excavation at Sukhothai Kilns June 11 - Sukhothai Historical Park (in Thai). Accessed 2 Nov 2021
- Sarjeant C (2014) *Contextualising the Neolithic occupation of Southern Vietnam: the role of ceramics and potters at An Son*. ANU Press, Singapore
- Shaw J (1981) *Northern Thai ceramics*. Oxford University Press, Malaysia

- Shaw J (1984) Northern Thai ceramics, a report of recent finds at Kalong, Nan, Sansai. *Payao and Chiengsaen SPAFA Digest* 1980–1990(5):12–15
- Smedley R, Duller G, Rufer D, Utley J (2020) Empirical assessment of beta dose heterogeneity in sediments: implications for luminescence dating. *Quaternary Geochronol* 56:101052. <https://doi.org/10.1016/j.quageo.2020.101052>
- Smith B, Rhodes E, Stokes S, Spooner N (1990) The optical dating of sediments using quartz. *Radiat Prot Dosimet* 34:75–78
- Srisuchat T (1996) Geological and archaeological expeditions in Thailand related to the maritime silk route. *Ancient Trades and Cultural Contacts in Southeast Asia*. Bangkok: The Office of the National Cultural Commission. 219–236.
- Srisum-Ang S, Panom S, Meetem T (1994) Mueang Nan, archeology, history and art (in Thai). Chuan Pim, Bangkok
- Stargardt J (2014) Indian Ocean trade in the ninth and tenth centuries: Demand, distance, and profit. *S Asian Stud* 30(1):35–55. <https://doi.org/10.1080/02666030.2014.892375>
- Steffen D, Preusser F, Schlunegger F (2009) OSL quartz age underestimation due to unstable signal components. *Quaternary Geochronol* 4:353–362. <https://doi.org/10.1016/j.quageo.2009.05.015>
- Stevenson J, Guy J (1997) *Vietnamese ceramics: A separate tradition*. Art Media Resources and Avery Press, Chicago
- Storm P, Wood R, Stringer C, Bartsiakos A, de Vos J, Aubert M, Kinsley L, Grün R (2013) U-series and radiocarbon analyses of human and faunal remains from Wajak. *Indonesia J Hum Evol* 64:356–365. <https://doi.org/10.1016/j.jhevol.2012.11.002>
- Sukkhama A (2018) Si Satchanalai figurines: reconstruction of ancient daily life, beliefs, and environment in Siam during the sixteenth century. *Int J Hist Archaeol* 22:800–842. <https://doi.org/10.1007/s10761-017-0449-7>
- Thansawangdumrong K (2005) The study of relationship between Muang Nan Sukhothai Lanna during the late 13th - 16th A.D. Evidence from Boh Suak Kiln Site (in Thai). Dissertation, Silpakorn University
- Tribolo C, Mercier N, Rasse M, Soriano S, Huysecom E (2010) Kobo 1 and L'Abri aux Vaches (Mali, West Africa): two case studies for the optical dating of bioturbated sediments. *Quaternary Geochronol* 5:317–323. <https://doi.org/10.1016/j.quageo.2009.03.002>
- Wallinga J (2002) Optically stimulated luminescence dating of fluvial deposits: a review. *Boreas* 31:303–322. <https://doi.org/10.1111/j.1502-3885.2002.tb01076.x>
- Wintle AG (1997) Luminescence dating: laboratory procedures and protocols. *Radiat Measur* 27:769–817. [https://doi.org/10.1016/S1350-4487\(97\)00220-5](https://doi.org/10.1016/S1350-4487(97)00220-5)
- Zacharias N, Michael C, Georgakopoulou M, Kilikoglou V, Bassiakos Y (2006) Quartz TL dating on selected layres from archaeometallurgical kiln fragments: a proposed procedure to overcome age dispersion. *Geochronometria* 25:29–35
- Zander A, Strebler D, Classen E, Rethemeyer J, Brückner H (2019) Roman traces in Germania magna: new thermoluminescence and pIRIR290 data from a lime kiln at Bergisch Gladbach, Germany. *Archaeometry* 61:506–518. <https://doi.org/10.1111/arcm.12435>
- Zuo X, Lu H, Zhang J, Wang C, Sun G, Zheng Y (2016) Radiocarbon dating of prehistoric phytoliths: a preliminary study of archaeological sites in China. *Sci Rep* 6:26769. <https://doi.org/10.1038/srep26769>

Publisher's note Springer Nature remains neutral with regard to jurisdictional claims in published maps and institutional affiliations.